The Canadian Mineralogist
Vol. 35, pp. 1325-1349 (1997)

PETROLOGICAL AND GEOCHEMICAL SIGNIFICANCE OF A DEVONIAN REPLACEMENT ZONE IN THE CAMBRIAN ROSEBERY MASSIVE SULFIDE DEPOSIT, WESTERN TASMANIA

KHIN ZAW[1], ROSS R. LARGE AND DAVID L. HUSTON*

Centre for Ore Deposits Research, Department of Geology, University of Tasmania, Hobart, Tasmania 7001, Australia

ABSTRACT

The Rosebery orebody is a polymetallic massive sulfide deposit hosted in felsic volcanic rocks of the Cambrian Mt. Read Volcanic belt, western Tasmania. The deposit underwent upper-greenschist-facies regional metamorphism and related deformation during the Devonian Tabberabberan Orogeny, resulting in folding, shearing, and faulting (thrusting) of the ore lenses. The south end of the Rosebery deposit has undergone metasomatic replacement related to the inferred intrusion of a post-orogenic Devonian granite, as interpreted from detailed gravity data. Mineralization at Rosebery consists of three primary sulfide–sulfate zones and a massive carbonate zone of Cambrian age: a lowermost pyrite – chalcopyrite zone (>4% Cu), an overlying sphalerite – galena ± pyrite zone, and an uppermost massive barite and carbonate zone. Devonian metasomatic mineral assemblages that overprint the south end of the orebody delineate three major zones: (1) magnetite – biotite ± chalcopyrite, (2) pyrrhotite – pyrite, and (3) tourmaline – quartz ± magnetite. Other metasomatic minerals, such as fluorite, garnet, and helvite, also are present in the Devonian assemblages. Field and textural relationships suggest that replacement of primary lead–zinc sulfide lenses occurred after folding. Magnetite – biotite ± chalcopyrite assemblages are confined to the lower levels of the mine, whereas pyrrhotite – pyrite and tourmaline – quartz ± magnetite assemblages occur toward the upper part of the orebody. No cross-cutting relationships between the pyrrhotite – pyrite zone and the magnetite – biotite ± chalcopyrite zone have been observed, suggesting that the minerals of these zones are products of a single evolving metasomatic event. The tourmaline – quartz ± magnetite assemblage seems to have formed late in the replacement process, as indicated by irregular and patchy quartz – tourmaline veins cutting the host rock and other sulfide lenses. Detailed underground examination also indicates that tourmaline – quartz veins demonstrably cut cleavage in the tuffaceous host-rocks, suggesting that the tourmaline veins formed after the development of the Devonian cleavage.

Keywords: Rosebery deposit, volcanogenic massive sulfide deposit, Devonian replacement, mineral chemistry, helvite, garnet, biotite, tourmaline, chlorite, Tasmania, Australia.

SOMMAIRE

Le gisement de Rosebery de sulfures massifs polymétalliques sont encaissés dans des roches volcaniques felsiques cambriennes de la ceinture du mont Read, en Tasmanie occidentale, Australie. Le gisement a subi les effets d'un métamorphisme régional dans le faciès schistes verts, ainsi qu'un épisode de déformation, au cours de l'orogenèse de Tabberabbera, ce qui a plissé, cisaillé, et déplacé par chevauchement les lentilles de minerai. Le secteur sud-est du gisement a en plus subi les effets d'un remplacement métasomatique, qui serait lié à la mise en place d'un granite dévonien post-orogénique. Le granite n'y est pas exposé, mais son existence à faible profondeur sous ce secteur est indiqué par un relevé détaillé de la gravité. La minéralisation est faite de trois zones primaires à sulfures + sulfates et d'une zone à carbonates massives, toutes d'âge cambrien: la zone inférieure, à pyrite + chalcopyrite (>4% Cu), ensuite une zone à sphalérite + galène ± pyrite, et une zone supérieure à barite massive, et la zone à carbonates. Les assemblages métasomatiques se répartissent en trois zones: (1) magnétite + biotite ± chalcopyrite, (2) pyrrhotite + pyrite, et (3) tourmaline + quartz ± magnétite. D'autres minéraux métasomatiques, tels fluorite, grenat et helvite, sont aussi présents. D'après les relations de terrain et les textures, les lentilles primaires à sulfures de Pb–Zn ont été remplacées après la déformation. Les assemblages à magnétite + biotite ± chalcopyrite sont restreints aux niveaux inférieurs, tandis que les assemblages à pyrrhotite + pyrite et à tourmaline + quartz ± magnétite sont développés dans la partie supérieure du gisement. Les assemblages 1 et 2 ne semblent pas se recouper, ce qui fait penser que ces minéraux se sont formés lors d'un seul événement en évolution. L'assemblage 3 est considéré tardif, comme en témoignent des veines irrégulières et discontinues à quartz + tourmaline qui recoupent les roches-hôtes et les autres lentilles de sulfures. D'après nos observations détaillées dans la mine, ces veines recoupent même le clivage des roches-hôtes tuffacées, et donc seraient post-déformation. Les analyses à la microsonde électronique montrent que le grenat a une forte composante de spessartine (74–85%, base molaire), avec grossulaire entre 3 et 15%. La helvite contient jusqu'à 7.0% de Zn (base pondérale). La biotite contient entre 1.81 et 2.73

* Present address: Geology and Geophysics, Australian Geological Survey Organisation, Canberra, ACT 2601, Australia.
[1] *E-mail address*: khin.zaw@utas.edu.au

atomes de ^{IV}Al par unité formulaire (*apuf*), et entre 0.02 et 2.75 *apuf* de ^{VI}Al; les valeurs de $100Mg/(Mg + Fe^{2+})$ vont de 22 à 54. Les compositions du grenat, de la helvite et de la biotite ressemblent à celles des gisements à W–Sn–F de Mt. Lindsay et de Cleveland en Tasmanie occidentale, formés par remplacement et aussi affiliés à des massifs de granite dévoniens. Le schorl, tourmaline dominante, est comparable à la tourmaline du granite dévonien de Meredith, mais il est plus riche en Fe que la plupart des compositions observées dans le gisement de sulfures massifs de Kidd Creek, en Ontario, et que toutes les compositions de tourmaline des gisements de la ceinture Appalachienne – Calédonienne. L'origine de la tourmaline et les autres minéraux des assemblages de skarn à Rosebery serait exclusivement liée à la mise en place d'un massif granitique.

(Traduit par la Rédaction)

Mots-clés: gisement de Rosebery, gisement volcanogénique de sulfures massifs, remplacement dévonien, composition des minéraux, helvite, grenat, biotite, tourmaline, chlorite, Tasmanie, Australie.

Introduction

Rosebery is the largest polymetallic volcanic-rock-hosted massive sulfide (VHMS) deposit known in western Tasmania. To date, it has produced 17.6 Mt at an average grade of 15.1% Zn, 4.6% Pb, 0.7% Cu, 152 ppm Ag, and 2.8 ppm Au; proven ore reserves are 4.0 Mt at 11.2% Zn, 3.6% Pb, 0.5% Cu, 127 ppm Ag, and 2.2 ppm Au (Mark Berry, pers. comm., 1995). Rosebery has a deformed sheet-like morphology and is hosted in felsic volcanic rocks of the Cambrian Mt. Read Volcanic Belt. The Mt. Read volcanic suite contains several other massive sulfide orebodies, including Hercules, Mt. Lyell, Hellyer, and Que River (Fig. 1).

The Rosebery deposit underwent upper-greenschist-facies regional metamorphism and associated deformation during the Devonian Tabberabberan Orogeny. In addition, the southern end of the Rosebery deposit has undergone metasomatic replacement related to an inferred intrusion of post-orogenic Devonian granite. Although the effects of Devonian processes on the Rosebery deposit were noted in the late 1960s, only a brief description of the recrystallization of sulfide ores (*e.g.*, Brathwaite 1969) and a short account of chemical remobilization of ore constituents during the Devonian (Solomon *et al.* 1987) have been presented.

In this paper, we document the geology, zoning, textures and petrology, and mineral chemistry of the Devonian assemblages in the F(J) lens of the Rosebery mine, and discuss their paragenesis and hydrothermal evolution in relation to the Cambrian VHMS assemblages. Physicochemical characteristics of the Devonian hydrothermal fluids, and chemical and thermodynamic aspects of the remobilization of ore constituents, are presented in a separate paper (Khin Zaw *et al.* 1997).

Regional Geological Setting

The regional geological and metallogenic relationships of the Rosebery–Hercules area and the Mt. Read volcanic sequence in western Tasmania have been extensively studied in recent years (*e.g.*, Corbett 1981, 1992, Corbett & Lees 1987, Corbett *et al.* 1989). Therefore, only the important geological relationships of the Rosebery area are presented in this paper.

The Rosebery deposit occurs within an arcuate, north–south-trending belt of Cambrian volcanosedimentary rocks between Precambrian blocks to the east and west. This belt contains volcanically derived sediments of the Dundas Group to the west, and the Mt. Read volcanic suite that host the Rosebery deposit to the east (Fig. 1). The Mt. Read volcanic suite is composed predominantly of rhyolite, dacite, and andesite, with minor basalt.

Following deformation and metamorphism during the Devonian Tabberabberan Orogeny, intrusion of shallow-level, post-orogenic granitic plutons in the mine area resulted in recrystallization and considerable modification of ore assemblages. Possible granite-related mineral assemblages including pyrrhotite, pyrite, garnet, helvite, biotite, and tourmaline were developed in the south-end orebody (Solomon *et al.* 1987). The Devonian granite does not crop out, but its presence has been inferred on the basis of detailed gravity data, at a depth of about one kilometer below the southern end of the deposit (Leaman & Richardson 1989).

Geology of the Rosebery Mine

Comprehensive accounts of the geology of the Rosebery area have been given by many previous investigators (*e.g.*, Brathwaite 1969, 1974, Burton 1975, Adams *et al.* 1976, Green *et al.* 1981, Green 1983, Lees *et al.* 1990), and only the major features are discussed here.

Stratigraphy

Major rock units in the Rosebery mine area include: (1) the Central Volcanic Complex (CVC) of the Mt. Read volcanic suite, (2) the Dundas Group, and (3) the Crimson Creek Formation (Fig. 1). The CVC in the mine area is faulted against the sedimentary rocks of the Dundas Group and sedimentary and mafic volcanic rocks of the Crimson Creek Formation. Recent drilling

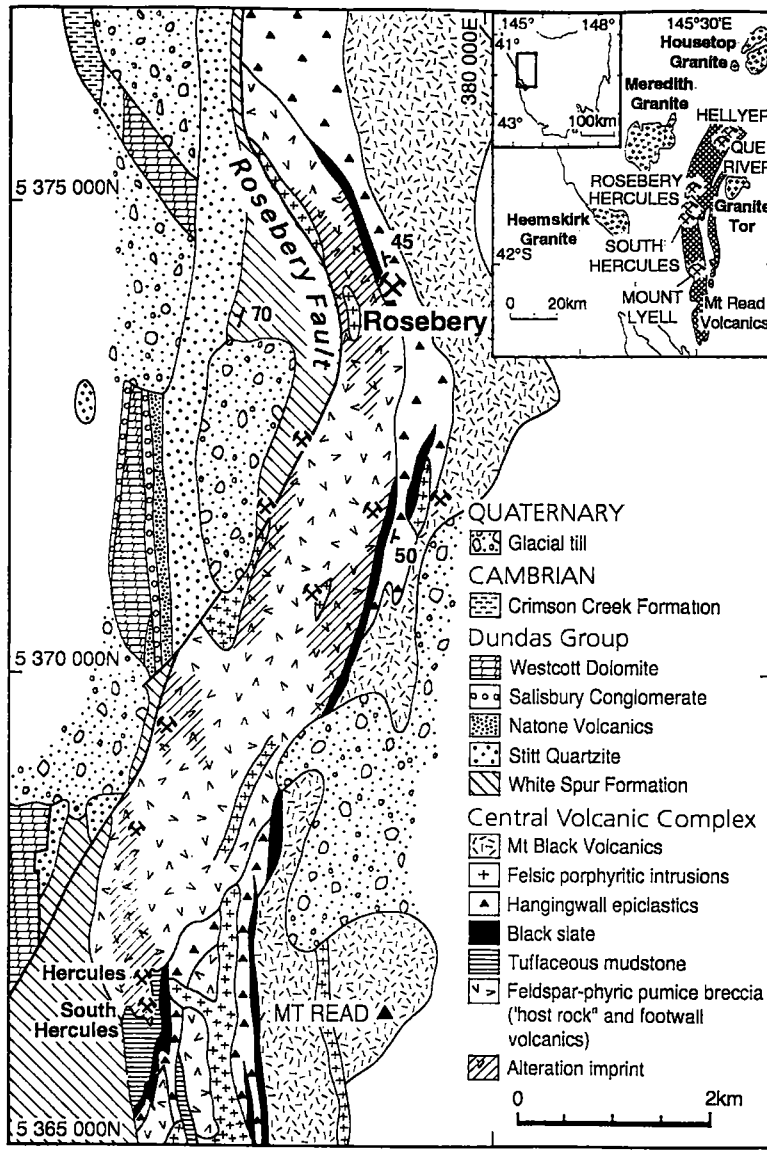

FIG. 1. Location and geological setting of the Cambrian Rosebery deposit, western Tasmania. Note the distribution of Devonian granitic intrusions in the inset.

has shown that the fault plane lies some 400 m beneath the Rosebery orebody (Corbett & Lees 1987). The CVC can be subdivided into the following stratigraphic units at the Rosebery mine:

Top	Mt. Black volcanic suite (dacitic to andesitic lavas)	>1000 m
	Hanging-wall epiclastic rocks	50–200 m
	Black slate	0–30 m
	Host rock: tuffaceous shale	35 m
Bottom	Footwall volcanic rocks (feldspar-phyric)	>300 m

The Rosebery deposit lies in a lens of tuffaceous shale at the contact between the footwall volcanic rocks and the hanging-wall epiclastic rocks. The footwall volcanic rocks consist of feldspar-phyric, ashy, vitric to crystal-rich tuffaceous rocks. Immediately below the Rosebery ore horizon, this unit has been altered to quartz – sericite – chlorite schist. The contact between the footwall volcanic rocks and the host rock typically

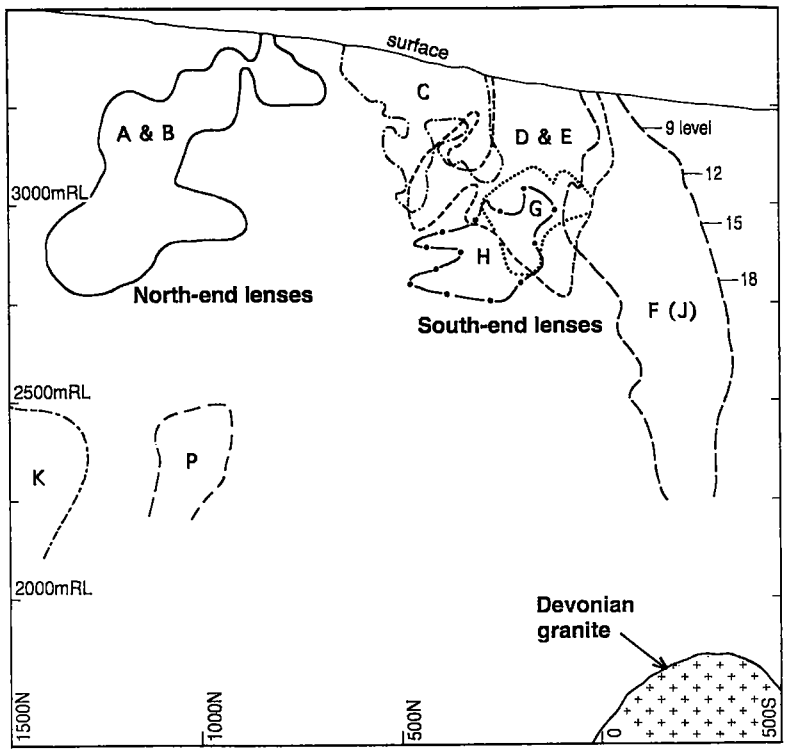

FIG. 2. Longitudinal section of Rosebery deposit, showing north-end ore lenses (A, B and newly discovered K and P) and south-end ore lenses (C, D, E, F-J, G and H). The position of the Devonian granite is interpreted from gravity data.

is difficult to distinguish in the mine area owing to the overprint of hydrothermal alteration.

The tuffaceous shale is commonly siliceous and sericitic, with disseminated pyrite. The host rock is locally chloritic and strongly sheared, with recrystallized pyrite cubes up to 5 cm across, and is overlain by up to 30 m of pyrite-bearing black slate. The shale and the overlying slate are considered to represent a period of quiet sedimentation during ore deposition (Green *et al.* 1981).

The hanging-wall epiclastic rocks consist of sericitized quartz–feldspar-phyric epiclastic sandstones and breccias. The presence of the assemblage albite – chlorite – quartz – epidote (Corbett & Lees 1987) in the hanging-wall epiclastic rocks indicates a lower-greenschist-facies metamorphic grade. These rocks are conformably overlain by the Mt. Black volcanic suite, which is composed of weakly sericitized and chloritized dacitic to rhyolitic lavas over 1000 m thick.

The Dundas Group, which unconformably overlies the CVC, consists of several subunits in the Rosebery–Hercules mine area: (1) the White Spur Formation, a quartz-phyric epiclastic sequence, (2) the Stitt Quartzite, (3) the Natone volcanic suite, (4) the Salisbury Conglomerate, and (5) the Westcott Dolomite. The Crimson Creek Formation is exposed in the western part of the Rosebery–Hercules area, tectonically interfingering with the Dundas Group. The Crimson Creek Formation consists of mafic greywacke interbedded with siltstone, mudstone, and minor altered basalt.

Structure

The Rosebery Fault is a prominent structure in the Rosebery–Hercules area. The fault dips east 30°–40°, and is characterized by a pyritiferous quartz–tourmaline vein-breccia in the Rosebery area, and a fault breccia elsewhere. It is interpreted to be a thrust fault with significant throw, as it juxtaposes east-dipping feldspar–phyric rocks of the CVC against steeply dipping, west-facing rocks of the Dundas Group (Corbett & Lees 1987). Shearing also has been noted in the ore lenses and the host rocks that are subparallel to the Rosebery Fault system (Berry 1990). Aerden (1991) also recognized reverse bedding-parallel shearing of

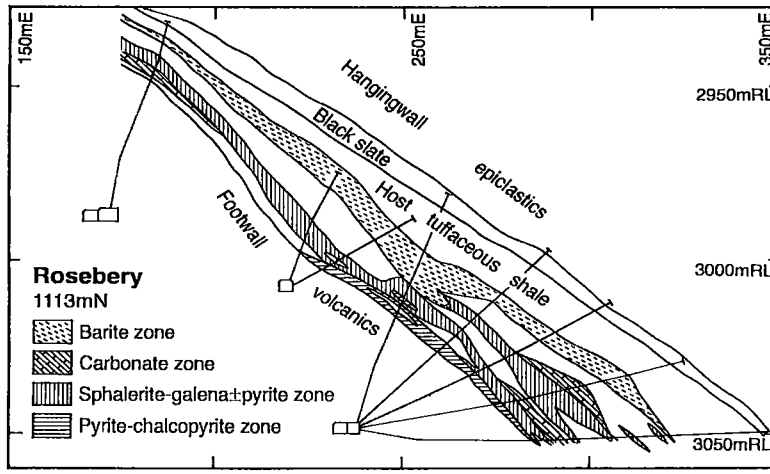

FIG. 3. Geology and mineral zonation, Rosebery north-end orebody.

the ore lenses and host rock, although he disagreed with a volcanogenic origin for the deposit.

Form and geometry of the ore lenses

The Rosebery orebody is made up of a series of tabular sheets that dip 45° east. The ore lenses extend over a strike length of 1.5 km to depths of at least 800 m at the south end and 600 m at the north end of the mine. A gap without economic mineralization separates the northern lenses from the main southern group of lenses (Fig. 2). Brathwaite (1969, 1972) first interpreted the folding of the Rosebery ore lenses as being due to the Devonian Tabberabberan Orogeny; a similar conclusion was reached by Green *et al.* (1981), Green (1983), and Lees *et al.* (1990). Adams *et al.* (1976) inferred that the folded structure resulted from synsedimentary slumping soon after ore deposition. However, Berry (1990) argued that the morphology of the lenses is due to a thrust duplex, with no mine-scale folding involved.

Mineralization and alteration

Base-metal mineralization that formed during Cambrian volcanic activity at Rosebery is mineralogically simple. The stratiform massive sulfide ore consists predominantly of pyrite, sphalerite, galena, chalcopyrite, and tetrahedrite–tennantite, with widespread minor arsenopyrite. Barite occurs at the stratigraphic top of the orebody, and commonly is separated from the sphalerite – galena ± pyrite ore by intervening barren host-rocks.

Barite-rich ore is generally of lower grade than zinc–lead ore, but contains essentially the same sulfide minerals, in slightly different proportions. Compared to sphalerite – galena ± pyrite ore, massive barite ore is characterized by an enrichment in galena and tetrahedrite–tennantite (Brathwaite 1969, 1974, Huston & Large 1988, Huston, 1989). Disseminated to massive pyrite mineralization with minor base-metals may occur distally from, or stratigraphically above, zinc–lead mineralization. The highest gold grades occur close to the stratigraphic hanging-wall of the deposit, in the upper part of the zinc–lead or barite-rich ore zones (Huston & Large 1988, Huston 1989).

The dominant feature of Cambrian alteration at Rosebery is a blanket-like zone of sericitic and chloritic assemblages in the footwall (*e.g.*, Green *et al.* 1981, Naschwitz 1985). The host rocks, originally tuffaceous siltstone and shale, are also altered to quartz – sericite – pyrite ± chlorite ± carbonate schists. Mineralogical changes that characterize this footwall alteration are destruction of feldspar, sericitization of pumice fragments, and silicification and pyritization of the groundmass. Where alteration is intense, a well-defined schistosity gives rise to an augen texture typical of "quartz schist", which commonly extends for several meters below mineralization into the footwall.

MINERALOGICAL ZONATION

Brathwaite (1969) first recognized a distinct stratigraphic zonation of ore-mineral assemblages at Rosebery. The stratigraphic zonation in ore constituents established by Brathwaite (1969, 1974), Green *et al.* (1981) and Green (1983) is similar to that recognized from many other volcanogenic massive sulfide deposits (*e.g.*, Stanton 1972, Franklin *et al.* 1981, Lydon 1984, 1988, Large 1977, 1992). Detailed mineralogical and zonation studies at the north end of the Rosebery deposit by Huston & Large (1988) have documented

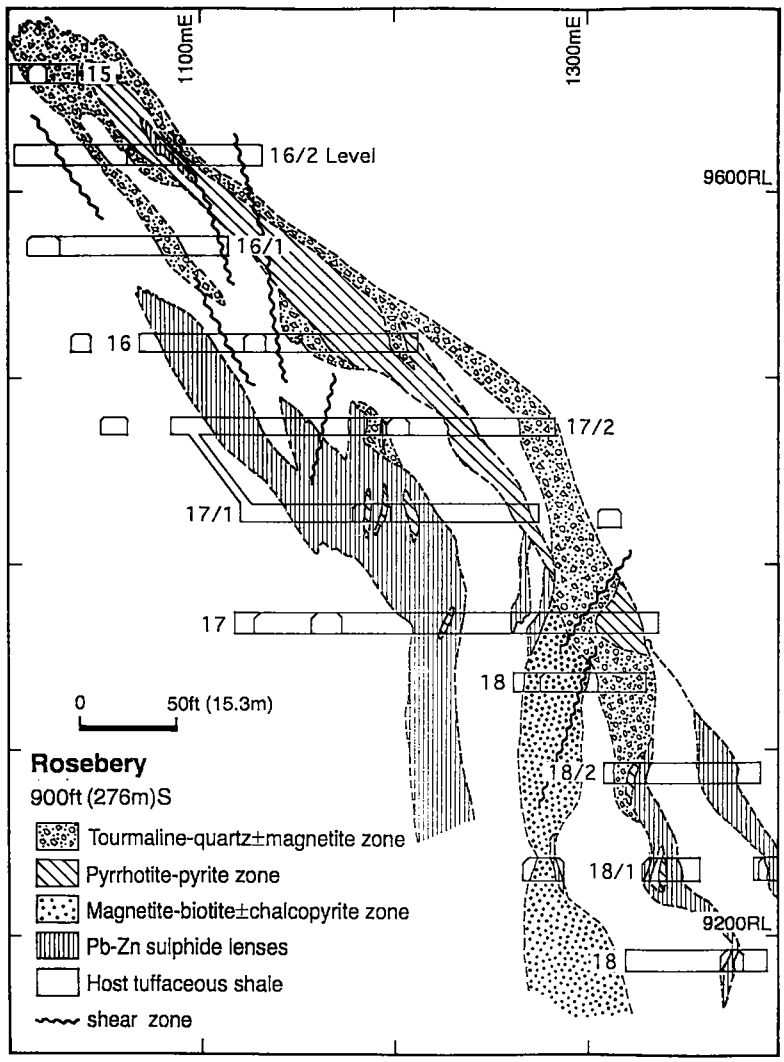

FIG. 4. Geological cross-section of Fe–S–O replacement assemblages, Rosebery south-end orebody.

the following primary sulfide–sulfate and carbonate zones (Fig. 3):

STRATIGRAPHIC TOP

Carbonate zone

Massive barite zone

Sphalerite – galena ± pyrite zone

Pyrite–chalcopyrite zone with Cu-rich pods (>4% Cu)

STRATIGRAPHIC BOTTOM

At the south end, the stratiform massive sulfide lenses are overprinted by a transgressive zone comprising iron oxides, sulfides and silicate minerals. Brathwaite (1969) first reported that the pyrrhotite-bearing assemblages transgress the sulfide lenses. Recent deep drilling in this area has exposed an extensive zone of pyrrhotite- and magnetite-bearing sulfide lenses. In addition to pyrrhotite, other secondary assemblages have been recognized, including magnetite (hematite) – biotite, pyrrhotite–pyrite, and tourmaline–quartz. Fluorite, garnet, and helvite also have been observed.

Underground-level plans and core logging illustrate the spatial distribution and zonation of the transgressive

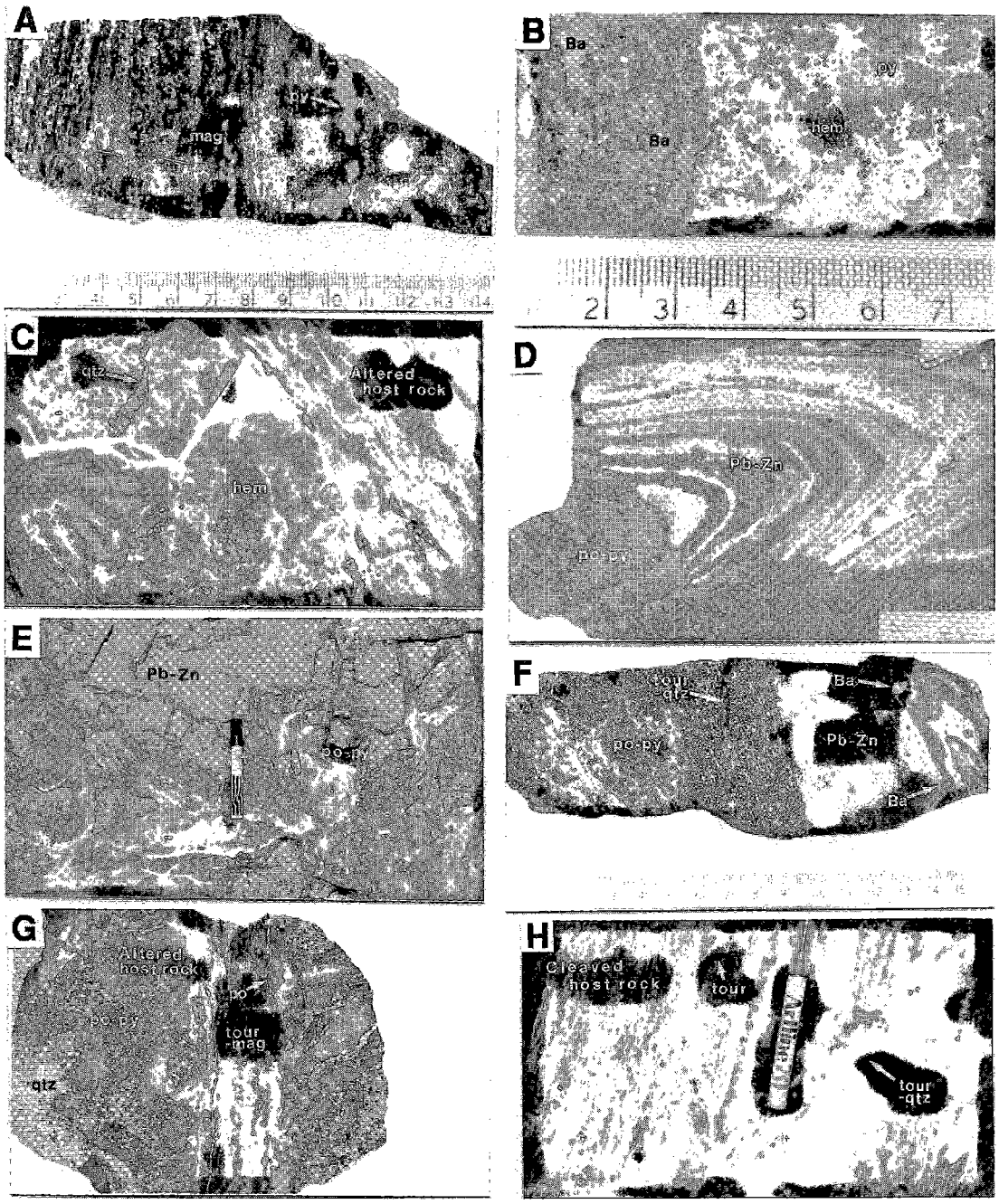

FIG. 5. Hand-specimen and underground photographs of Rosebery ores. A. Pyrite – magnetite assemblages showing pseudo-banded texture, F(J) lens. B. Hematite – pyrite in contact with barite – pyrite assemblages, F(J) lens. C. Underground exposure of hematite ± quartz assemblages, H lens. D. Folded lead – zinc ore and pyrrhotite and pyrite assemblages, south-end orebody. Scale bar is 4 cm. E. Underground exposure of pyrrhotite – pyrite assemblages, F(J) lens. F. Pyrrhotite – pyrite assemblages and Pb – Zn sulfide ores, F(J) lens. G. Tourmaline – quartz vein cutting pyrrhotite–pyrite assemblages, F(J) lens. H. Underground exposure of tourmaline – quartz vein, F(J) lens, south-end orebody.

Fe–S–O assemblages. Detailed zonal patterns of the Fe–S–O assemblages and their relationship to the Pb–Zn lenses on eleven east–west cross-sections from the south-end were investigated (Khin Zaw *et al.* 1988). Figure 4 shows the spatial distribution and zonation on the scale of the orebody. The following three major zones can be distinguished: 1) magnetite – biotite ± chalcopyrite zone, 2) pyrrhotite – pyrite zone, and 3) tourmaline – quartz ± magnetite zone.

Magnetite – biotite ± chalcopyrite zone

This zone is generally confined to the lower levels of the mine, particularly below 17 Level. Magnetite forms massive bodies with pyrite and biotite. The pyrite – magnetite ± biotite assemblages may show a pseudobanded texture (Fig. 5A). Pyrite commonly occurs as cubes of various size in the magnetite ± biotite host. Hematite is locally noted with magnetite; in places, only hematite is found with pyrite; it also occurs in barite-rich sulfide lenses (Fig. 5B). Hematite ± quartz zones up to half a meter across (Fig. 5C) locally occur within biotite-rich alteration associated with magnetite assemblages.

Biotite in this zone is massive, mottled, and green to dark green in color. Chlorite occurs in the sulfide lenses and the footwall, and is associated with biotite. Sericite and K-feldspar are also found in this zone. Recrystallized chalcopyrite is abundant. Garnet – biotite and garnet – helvite – tourmaline assemblages are present in this zone at deeper levels of the mine.

Pyrrhotite – pyrite zone

Zones of pyrrhotite – pyrite extend from 14 Level down to 17 Level, where they give way to magnetite-rich assemblages. Brathwaite (1974) first reported that pyrrhotite – pyrite assemblages transgress folded primary Pb–Zn sulfide lenses (Figs. 5D, E, F). Most of the sphalerite and galena in the banded sulfides is replaced by pyrrhotite and pyrite; only thin sphalerite-rich bands remain, retaining the folded structure (Fig. 5D). Major zones of pyrrhotite – pyrite bodies cut the Pb–Zn sulfide lenses in the F(J) lens along 16 No. 2 Sub-Level, 16 Level, 17 No. 2 Sub-level, and 17 Level.

Massive pyrrhotite – pyrite bodies range from 1 m to more than 20 m across. A zone of dark brown, coarse-grained sphalerite is common as a rim between massive pyrrhotite – pyrite and original sphalerite – galena lenses. As described by Solomon *et al.* (1987), this pyrrhotite – pyrite zone varies from pyrrhotite-dominant to pyrite-dominant with or without tourmaline, magnetite, and biotite. No large bodies of pyrrhotite – pyrite were observed below 17 Level, although thin lenses of pyrrhotite – pyrite with chalcopyrite occur in the massive magnetite – biotite zone.

TABLE 1. MINERAL ASSEMBLAGES FOUND AT THE ROSEBERY DEPOSIT, ACCORDING TO TYPE OF MINERALIZATION

	Massive pyrite – chalcopyrite	*Massive sphalerite – pyrite – galena*	*Massive barite*
Major	Pyrite and chalcopyrite	Sphalerite, galena, and pyrite	Sphalerite and galena
Minor to trace	Sphalerite, galena, arsenopyrite, tennantite, magnetite, aikenite, kobellite, cosalite, bismuth, pyrrhotite, and electrum	Chalcopyrite, arsenopyrite, tetrahedrite, magnetite, electrum, bournonite, boulangerite, meneghinite, miargyrite*, pyrargyrite, enargite, argentite, and cubanite*	Pyrite, chalcopyrite, tetrahedrite, electrum, pyrargyrite, bournonite, sulvanite*, and native lead*
Gangue	Chlorite and quartz, with lesser carbonate and sericite	Chlorite, quartz, carbonate and sericite, with minor albite and trace celsian*	Barite, quartz, albite, sericite, and carbonate

	Devonian gash veins	*Devonian metasomatic assemblages*
Major	Galena, chalcopyrite, sphalerite, and pyrite	Pyrrhotite, pyrite, magnetite, chalcopyrite, and hematite
Minor	Tetrahedrite, meneghinite, bournonite, jordanite, electrum, molybdenite, cassiterite, stannite, bismuthinite, native bismuth, gold, maldonite, and ullmannite*	Tetrahedrite, bismuth, electrum, and wolframite
Gangue	Quartz and carbonate	Garnet, helvite, tourmaline, fluorite, chlorite, quartz, and biotite

* Reported for the first time in this study.

Tourmaline – quartz ± magnetite zone

The tourmaline – quartz zone envelops and overprints the massive pyrrhotite – pyrite zone. It is well exposed at the southernmost end of the F(J) lens. This zone consists of irregular and patchy quartz – tourmaline veins that cut the host rock and other sulfide lenses (Fig. 5G). The tourmaline in this zone commonly forms networked, banded, thin veinlets. The tourmaline – quartz veins clearly postdate the cleavage in the tuffaceous host-rocks (Fig. 5H). Although tourmaline and quartz are the dominant minerals in this zone, patches of pyrrhotite, pyrite, and magnetite (± hematite) with minor chlorite, fluorite, and carbonates also were noted.

Mineralogy and Textures

Table 1 summarizes the mineralogy of volcanogenic ores at Rosebery.

Ores formed from Cambrian volcanogenic fluids

Pods of banded *massive pyrite – chalcopyrite* occur along the footwall contact of the massive sulfide lenses. Minor minerals include sphalerite, galena, arsenopyrite, and tennantite; trace minerals are kobellite, aikinite, native bismuth, pyrrhotite, and electrum. Native

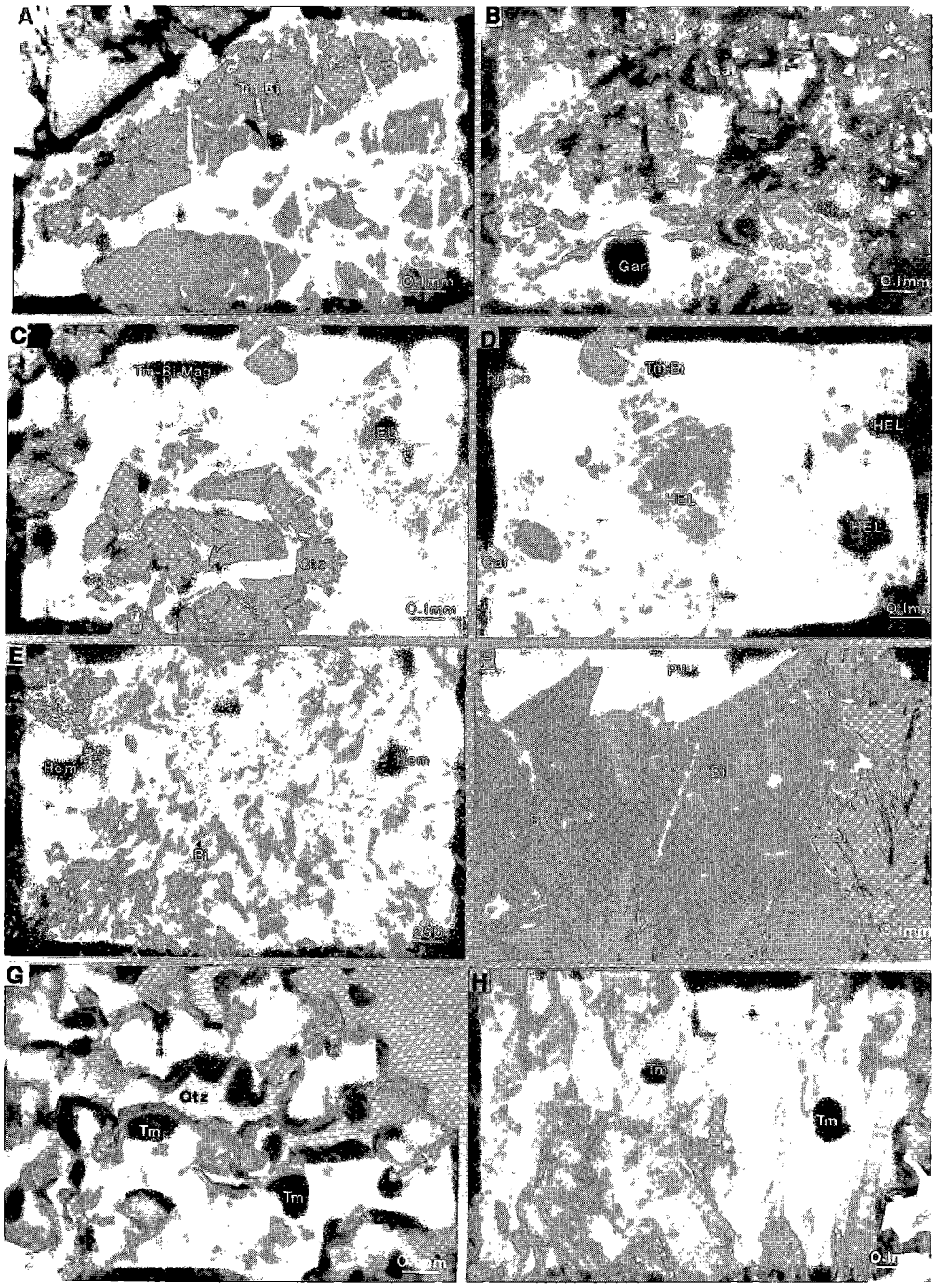

FIG. 6.A. Garnet grain cut by tourmaline–biotite veinlets. B. Same as above under crossed nicols. C. Subhedral grain of garnet together with wedge-shaped crystal of helvite, biotite and tourmaline. D. Helvite crystals together with altered anhedral to subhedral grains of garnet. E. Flakes of biotite with hematite. The biotite appears to have been altered from chlorite. F. The association of biotite + pyrite. G. Euhedral crystals of zoned tourmaline in matrix of quartz. H. Prismatic, bladed tourmaline forming 3 – 5 cm-thick layers of tourmaline layers of tourmalinite assemblage, F(J) lens, southend of Rosebery mine, western Tasmania.

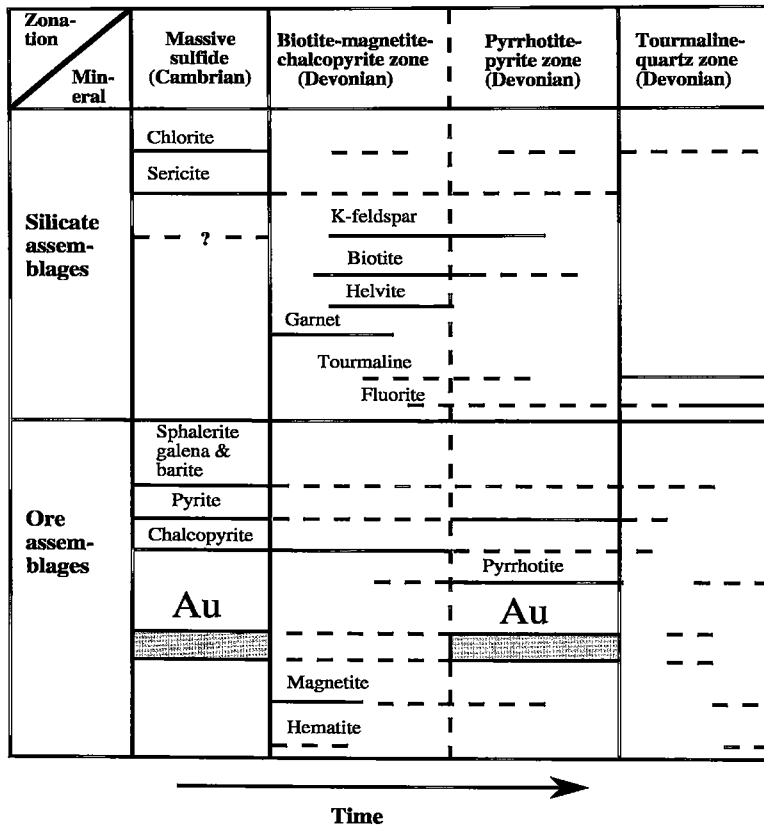

FIG. 7. Schematic diagram showing paragenetic relationships of assemblages of replacement minerals in the F(J) lens, south-end orebody. Evidence used for the paragenetic relationships includes microtextural and macrotextural data.

bismuth, bismuth sulfosalts, and pyrrhotite occur with birds-eye pyrite in chalcopyrite. Chlorite and quartz are the most common gangue minerals; lesser sericite and carbonate also are present. Chlorite and sericite are generally foliated parallel to banding, whereas quartz and carbonate occur as anhedral grains, with carbonate typically forming polycrystalline aggregates.

Well-banded *massive sphalerite – galena – pyrite*, which forms most of the ore, also contains minor chalcopyrite, arsenopyrite, and tetrahedrite. Ron F. Berry (pers. comm., 1990) has suggested that the fine-scale banding (1–10 mm) is probably tectonic, whereas the coarser banding may be primary. The mineral textures, typical of deformed sulfide ores (Stanton 1972), comprise porphyroblastic pyrite and annealed intergrowths of sphalerite, galena, and other sulfides. Minor colloform and framboidal pyrite also is present (Brathwaite 1974, Green *et al.* 1981). A "snowflake" intergrowth between pyrite and other sulfide minerals is interpreted as a primary texture caused by the rapid coprecipitation of pyrite with other sulfide minerals. Miargyrite and cubanite are recorded for the first time at Rosebery; boulangerite and meneghinite are recorded for the first time in fine-grained massive sphalerite – pyrite – galena ores. Miargyrite occurs in Ag-rich samples with pyrargyrite, bournonite, and galena; cubanite occurs with chalcopyrite. Boulangerite and meneghinite form inclusions in pyrite. Boulangerite also occurs as lath-like grains associated with chalcopyrite and galena, and meneghinite occurs with bournonite.

The gangue minerals are mainly chlorite, quartz, carbonate, and sericite, with minor albite and trace celsian. Albite is concentrated in the lateral and upper portions of the deposit; it is particularly abundant in samples from the north-end orebody. Celsian (approximately $Ba_{0.75}K_{0.25}Al_{1.75}Si_{2.25}O_8$) occurs as 0.1–0.5 mm subhedral grains that are overgrown by albite; it contains inclusions of sulfides, and is dusted by sericite. Celsian is uncommon in VHMS ores, having

been reported only at the Tulks Hill deposit in Newfoundland (McKenzie *et al.* 1993). Barian feldspar occurs more commonly in sediment-hosted massive sulfide deposits (*e.g.*, Segnit 1946, Lydon *et al.* 1982, Fortey & Beddoe-Stephens 1982).

The most common sulfide minerals present in lenses of *massive barite* are sphalerite and galena, accompanied by lesser pyrite, chalcopyrite, and tetrahedrite. Barite-rich lenses have a lower abundance of pyrite, a higher abundance of tetrahedrite, and lack arsenopyrite relative to massive sphalerite – pyrite – galena ores (Brathwaite 1974, Green *et al.* 1981). They also are banded, and locally brecciated, with subangular fragments of sugary massive barite set in a sulfide matrix.

Trace minerals in the lenses of massive barite include electrum, bournonite, sulvanite (Cu_3VS_4), and native lead; the sulvanite and native lead were observed at Rosebery for the first time in this study. Sulvanite, which also is a trace mineral in some Kuroko deposits in Japan (Matsukuma *et al.* 1974, Shimazaki 1974), occurs as 10–50 μm inclusions in sphalerite. Native lead forms a rim around a grain of tetrahedrite in contact with galena. Less abundant gangue minerals include quartz, albite, sericite, carbonate, and trace chlorite (Green *et al.* 1981).

Ores formed during Devonian recrystallization and metasomatism

During Devonian lower-greenschist-grade metamorphism, the ore assemblages were recrystallized to produce most of the observed textures. Associated with this metamorphism, minor remobilization of ore formed quartz – carbonate gash veins that commonly contain complex sulfide assemblages in the vicinity of lenses of massive sulfide or barite. Massive sulfide and barite-rich ores in the southern end of the deposit were replaced by pyrrhotite – pyrite, magnetite – pyrite, and pyrite – hematite assemblages during metasomatism associated with the inferred intrusion of a post-orogenic Devonian granite.

Quartz – carbonate gash veins that formed during Devonian metamorphism typically contain abundant sulfide and sulfosalt minerals in the vicinity of the Rosebery orebodies. Many of the less common minerals identified by Williams (1960) were collected from this type of vein. The most abundant sulfide minerals in the gash veins are sphalerite, galena, chalcopyrite, and pyrite, with lesser quantities of Ag-rich, end-member tetrahedrite. These veins also contain meneghinite, bournonite, jordanite, pyrargyrite, and electrum (Williams 1960, Brathwaite 1974, Huston & Large 1988). In addition to the above minerals, Williams (1960) observed inclusions of arsenopyrite, molybdenite, cassiterite, and stannite in a sample of massive tetrahedrite; Huston & Large (1988) reported the occurrence of a vein of bismuthinite – maldonite – native gold of probable Devonian age from the D lens. In this study, a 7-μm triangular inclusion of ullmannite (NiSbS) was observed in remobilized galena. The Devonian gash veins contain mainly a quartz and carbonate gangue, with lesser sericite and chlorite.

Devonian metasomatic assemblages recorded in the F(J) lens

Stillwell (1934) was the first to report spessartine-rich *garnet* at the Rosebery mine. This identification was later confirmed by Green *et al.* (1981) and Lees (1987), who attributed the garnet-bearing assemblage to postdepositional metamorphism. Garnet is typically found in the deeper levels of the F(J) lens. Garnet occurs as creamy white, anhedral gains in hand specimen, and is associated with pyrrhotite, pyrite, magnetite, biotite, tourmaline, and fluorite.

Under the microscope, the crystals of garnet may exceed 5 mm in diameter, and are pale orange or pale brown, commonly anisotropic and zoned, with or without penetration twinning (Figs. 6A, B, C). A few crystals show both anomalous anisotropism and pronounced zoning, but the coarsely crystalline subhedral aggregates show only weakly developed zoning, which is commonly parallel to crystal outlines. Some isotropic or nearly isotropic grains also are present. Garnet may be altered to helvite, and both minerals are cut by tourmaline – biotite veinlets or rimmed by prismatic tourmaline. In other samples, garnet-bearing assemblages are cut by quartz – carbonate – fluorite veins.

Crystals of helvite also occur in the deeper levels of the mine. Under the microscope, helvite from Rosebery is pink, rhombic in shape, and replaces garnet (Fig. 6C). Some grains are distinctly zoned (Figs. 6D), or are found in association with pyrite.

Biotite is commonly intergrown with magnetite. In hand specimen, it can easily be mistaken either for tourmaline or a dark green variety of chlorite. Pyrite euhedra are first replaced by hematite or magnetite and then by biotite – magnetite. In thin section, the color of biotite varies from green to brown. Biotite forms thin veinlets or flakes (Figs. 6E, F) and locally occurs as an alteration product of garnet (Figs. 6A, C, D).

Tourmaline was reported at the Rosebery mine by Finucane (1932), Stillwell (1934), Green (1983), Lees (1987), Plimer & Lees (1988), and Lees *et al.* (1990). Tourmaline is a ubiquitous mineral that cuts sulfide lenses and host rock in the south end of the mine; it occurs in thin veinlets or lenses. Plimer & Lees (1988) described 3–5-cm-thick layers of tourmaline (15 Level) as tourmaline exhalites, but recent field and microscopic investigations of the tourmaline assemblages, together with geochemical and isotopic evidence, do not support this interpretation (Khin Zaw 1991, Khin Zaw & A. Fallick, unpubl. data).

Tourmaline veinlets commonly cut helvite, garnet, and sulfide assemblages. Under the microscope, tour-

maline occurs as euhedral, prismatic, or stubby trigonal grains containing a dark green core and a pale green rim, or *vice versa* (Fig. 6G). Thin layers of prismatic tourmaline and veins also are present (Fig. 6H).

Chlorite is associated with sericite in the footwall alteration-zone. It also occurs intergrown with biotite and tourmaline. It shows a fine-grained felted appearance or forms coarse elongate "pressure shadow" grains next to sulfide minerals. Chlorite also occurs as an alteration product of biotite at the margin of fluorite-bearing retrograde veins in biotite – magnetite assemblages.

Sericite is a common alteration mineral at Rosebery. It may be found with K-feldspar, biotite, tourmaline, and garnet. K-feldspar occurs as minor irregular, anhedral aggregates. Various forms of carbonate minerals noted in the F(J) lens were described by Khin Zaw (1991).

Paragenesis and Timing of Replacement Assemblages

Mineralogical and cross-cutting relations among the replacement minerals discussed above indicate the following paragenetic sequence, from oldest to youngest: garnet → helvite → biotite – tourmaline → tourmaline → tourmaline – fluorite. The general paragenetic relationships of the dominant silicate minerals and their associated Fe–S–O assemblages in the F(J) lens are shown in Figure 7.

Garnet, helvite, biotite, and magnetite are concentrated in the biotite – magnetite ± chalcopyrite zone. Although tourmaline also occurs throughout this zone, it is most abundant in the tourmaline – quartz zone. The following microtextural relationships indicate that tourmaline nucleated after deformation, during the last stage of metasomatism: (1) most shear zones are filled with tourmaline – quartz veinlets, (2) tourmaline veinlets cut the sulfide assemblages, and (3) other silicate minerals (garnet, helvite, and biotite) in the replacement assemblages also are cut by tourmaline veinlets.

Textural relations suggest that the replacement of the primary massive sulfide lenses by the Fe–S–O assemblages occurred after folding and deformation of the Cambrian Pb–Zn sulfide lenses. For example, the pyrrhotite – pyrite assemblages clearly cut folds in the Pb–Zn ore (Figs. 5D). This evidence, together with the abundant post-cleavage tourmaline – quartz veining developed in the ore zone, indicates that the replacement occurred some time after the Tabberabberan Orogeny. Timing relationships preclude these metasomatic assemblages from being related to pre-orogenic Cambrian granites.

Magnetite extensively replaces lenses of massive pyrite to form massive bodies (with or without biotite) wherever replacement was complete. Pyrite can still be recognized in the magnetite ± biotite host, and the presence of coalesced pyrite cubes variably altered to magnetite suggest that the replacement occurred after the metamorphic (?) recrystallization of pyrite.

Primary Pb–Zn sulfides are separated from the pyrrhotite – pyrite zone by a reaction rim that contains Fe-rich sphalerite. The pyrrhotite – pyrite zone occurs mostly above the magnetite – biotite ± chalcopyrite zone (Fig. 4), and contains relict magnetite. A significant amount of gold is present in the pyrrhotite – pyrite zone (Khin Zaw 1991, Khin Zaw *et al.* 1997). No cross-cutting relations between the pyrrhotite zone and the magnetite zone have been observed, suggesting that these two Fe–S–O assemblages may be products of a single, evolving metasomatic event.

The tourmaline – quartz ± magnetite zone appears, in contrast, to have formed at a late stage during the replacement process, as evidenced by the occurrence of irregular and patchy quartz – tourmaline veins that cut the host rock and sulfide lenses. Although tourmaline – quartz veins seem to be stratiform and parallel to the bedding in drill-core intersections, recent detailed underground examination indicates that the tourmaline – quartz veins demonstrably cut the cleavage of the tuffaceous host-rocks (Fig. 5H), thus suggesting formation of the veins after the development of a Devonian cleavage.

Geochemistry of the Replacement Minerals

Compositional variations of garnet, helvite, biotite, tourmaline, chlorite, sericite, and K-feldspar were determined in this study. These compositions are compared here with data from the Cleveland and Mt. Lindsay replacement tin deposits (Devonian) in western Tasmania, and from the CanTung high-temperature skarn deposit in the Northwest Territories.

TABLE 2. REPRESENTATIVE COMPOSITIONS OF GARNET, F(J) LENS, ROSEBERY MINE, TASMANIA

Sample no.	88R-4A (14)	88R-6 (6)	R1920-12 (4)		88R-4A	88R-6	R1920-12
SiO_2 wt.%	34.30	34.60	34.74	Si	2.84	2.85	2.92
Al_2O_3	20.07	20.15	19.58	^{IV}Al	0.16	0.15	0.09
				^{VI}Al	1.80	1.81	1.86
TiO_2	0.27	0.19	0.25	Ti	0.02		0.02
FeO	5.93	5.04	6.44	Fe^{3+}	0.21	0.18	0.13
				Fe^{2+}	0.18	0.15	0.32
MnO	36.23	35.56	34.72	Mn	2.55	2.50	2.49
MgO	0.08	0.21	0.24	Mg	0.02	0.26	0.03
CaO	3.22	4.74	3.05	Ca	0.29	0.36	0.28
Total	100.10	100.49	99.02		8.07	8.26	8.14
Andradite	6.39	5.81	4.11				
Spessartine	79.22	78.20	77.26				
Almandine	5.52	4.72	10.01				
Grossular	8.87	11.28	8.62				
Sps + Alm	84.74	82.92	87.88				

The number of electron-microprobe analyses carried out is shown in parentheses. The structural formulae are calculated on the basis of 12 atoms of oxygen.

Analytical techniques

Chemical analyses of minerals were carried out using a JEOL JXA–50A electron microprobe employing an accelerating voltage of 20 kV, a beam current of 0.34×10^{-9}A, a beam diameter of 2–3 μm, and a counting interval of 120 seconds. Between two and five compositions were averaged to yield each composition reported here.

Garnet

Compositional data for garnet are given in Table 2. Although the iron content is reported as FeO, iron is partitioned to fill the R^{3+} sites in calculations of the structural formulae. The garnet consists predominantly of spessartine (74.2–84.9 mol.%) and minor grossular (3.2–16.1 mol.%). The almandine component ranges from 1.3 to 11.2 mol.%, whereas the andradite component varies from 2.8 to 11.2 mol.%. The Mg content of the garnet is uniformly negligible (<0.25 wt% MgO).

Compositions of garnet are compared (Fig. 8) with those from the Mt. Lindsay and Cleveland replacement deposits, Tasmania (Kwak 1983, Barth 1986) and from the high-temperature skarn at CanTung (Khin Zaw 1976). Compositions are similar to those of garnet from the Cleveland deposit. They differ from those of the high-temperature (to 520°C) tungsten skarn environment at the CanTung mine, in which the garnet contains a larger proportion of the grossular component (Khin Zaw 1976).

Similarity in the compositional ranges of garnet from the Rosebery and Cleveland deposits suggests similar metamorphic–metasomatic conditions. At Cleveland, a relatively low to moderate range of temperatures of mineralization has been reported from fluid-inclusion and stable-isotope studies (Collins 1981). Fluid-inclusion data also suggest moderate temperatures ($T_h < 330$°C) for formation of the replacement assemblages at Rosebery (Khin Zaw 1991). In contrast, the garnet from Mt. Lindsay contains very little spessartine and almandine component; it is grossular-rich, with considerable andradite component. The inferred temperature of the Mt. Lindsay W–Sn–F–Be skarns, based on mineral-equilibria studies, is greater than 400°C (Kwak 1983). The composition of garnet at Mt. Lindsay appears to have varied owing to fluctuations in temperature and other physicochemical conditions, such as $f(O_2)$.

Garnet is a nearly ubiquitous mineral in skarn deposits. In comprehensive reviews of skarns, Einaudi & Burt (1982) reported on the compositional range of garnet, and Meinert (1983, Fig. 2) related compositional variations of the garnet to various types of skarn. According to Meinert (1983), the composition of garnet from tin skarns is generally restricted to more

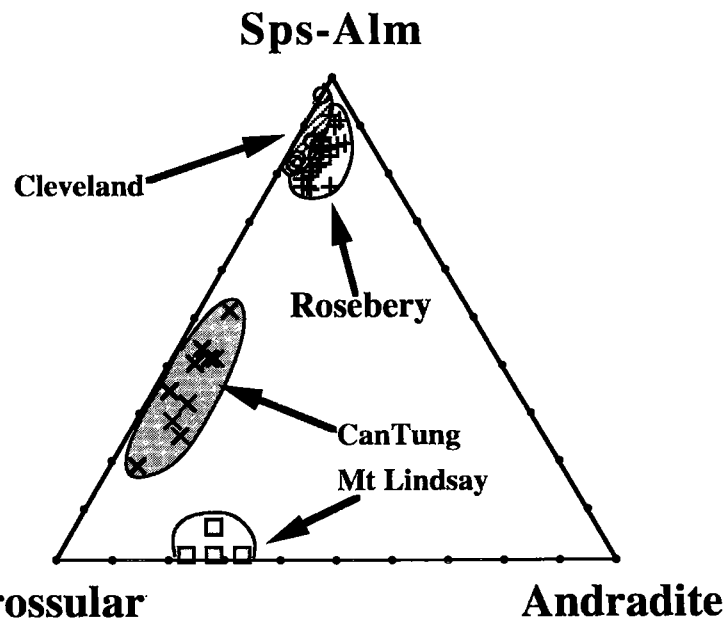

FIG. 8. Compositional variation of garnet at Rosebery together with that of garnet from Mt. Lindsay and Cleveland, western Tasmania (Kwak 1983, Barth 1986), and from the CanTung deposit, Northwest Territories, Canada (Khin Zaw 1976).

andraditic compositions, although it may have a significant grossular component. Garnet in tungsten skarns displays a wider compositional variation, and commonly is Fe- or Mn-rich, in some cases approaching the almandine or spessartine end-member. The composition of garnet from the F(J) lens at Rosebery shows combined almandine and spessartine components of 76.7 to 92.0 mol.%, comparable compositionally to that of some tungsten skarn deposits. The garnet at Rosebery contains less almandine component (5–10 mol. %) than the metamorphic garnet (17–80 mol. %) associated with massive sufide deposits, as reported by Spry (1990).

Newberry (1983) used the compositional variation of garnet from tungsten skarn deposits as a criterion for classification of the deposits into (1) strongly reduced, (2) moderately reduced, and (3) oxidized skarns:

	Strongly reduced skarn	Moderately reduced skarn	Oxidized skarn
Andradite mol.%	0–30	10–75	80–98
Spessartine mol.%	3–35	5–40	0–3
Almandine mol.%	3–40	2–35	0

According to Newberry's classification, the garnet from the F(J) lens of the Rosebery deposit falls in the strongly to moderately reduced class of tungsten skarn.

TABLE 3. REPRESENTATIVE COMPOSITIONS OF HELVITE, F(J) LENS, ROSEBERY MINE, TASMANIA

Sample no.	88R-6 (3)	17L-H (23)		88R-6	17L-H
SiO_2 wt.%	35.57	36.30	Si	3.66	3.69
Al_2O_3	0.81	0.68	Al	0.11	0.08
FeO	19.63	16.75	Fe^{2+}	1.69	1.44
MnO	26.79	31.82	Mn	2.34	2.73
ZnO	6.66	5.04	Zn	0.51	0.35
S	5.55	5.77	S	1.07	0.60
Total	95.01	96.36		9.38	8.89
Danalite	36.99	31.41			
Helvite	50.46	59.16			
Genthelvite	12.55	9.43			

The number of electron-microprobe analyses carried out is shown in parentheses. The structural formulae are calculated on the basis of 12 atoms of oxygen.

The garnet therefore probably formed under reducing conditions, although hematite is locally noted in the barite-rich massive sulfide lenses. Assay values up to 0.25 wt% WO_3 have been reported from the lower levels of the F(J) lens (S. R. Hunns, pers. commun., 1991), which supports a metasomatic skarn-type model for the origin of the garnet.

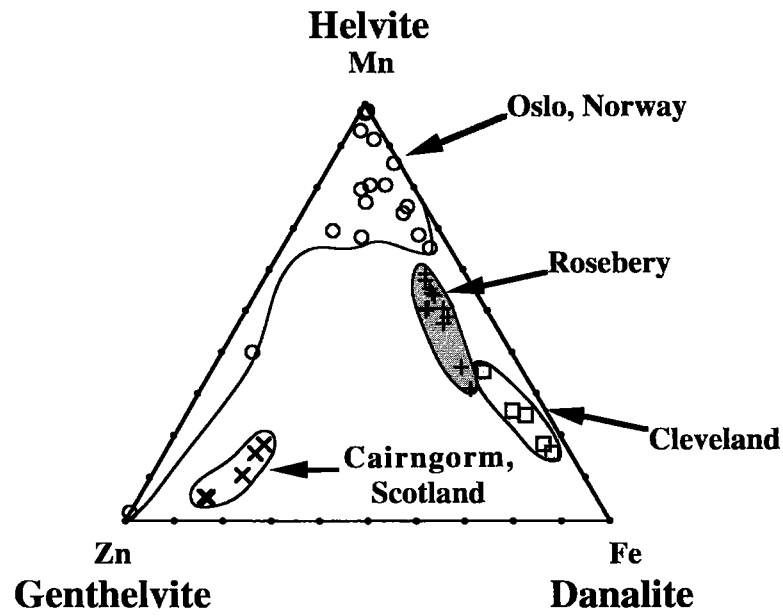

FIG. 9. Compositional variation of helvite – danalite at Rosebery together with that of helvite-group minerals from Cleveland, western Tasmania (Barth 1986), syenite pegmatite, Oslo region, Norway (Larsen 1988), and of genthelvite from the Cairngorm Mountains, Scotland (Clark & Feijer 1976).

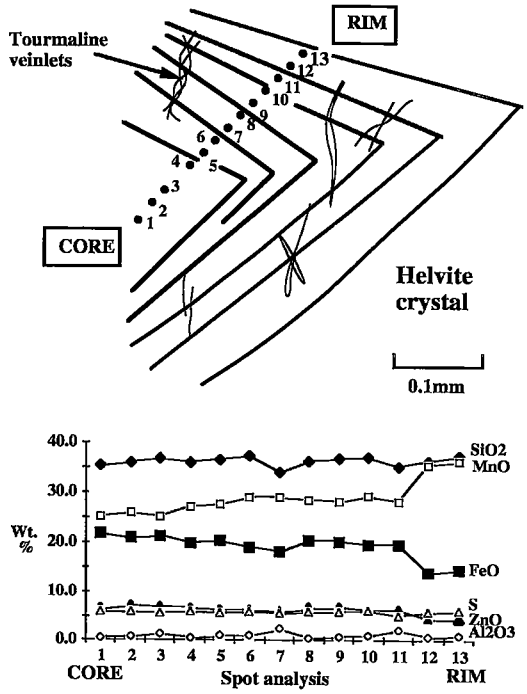

FIG. 10. Compositional variation within a single crystal of helvite from the F(J) lens, Rosebery south-end orebody.

Helvite-group mineral

Helvite-group minerals comprise beryllium- and sulfur-bearing silicates having the general formula $R_4Be_3(SiO_4)_3S$, where R = Mn (helvite), Fe^{2+} (danalite) or Zn (genthelvite). Results of electron-microprobe analyses are presented in Table 3. The proportion of beryllium could not be determined. The Rosebery material, with 7.0 wt% Zn, contains up to 55.7 mol.% danalite, and up to 13.0 mol.% genthelvite (Fig. 9). Analyses from core to rim across a wedge-shaped crystal indicate no major changes in composition, apart from a slight enrichment in Mn at the expense of Fe^{2+} at the rim (Fig. 10).

Occurrences of helvite and danalite have been described by many authors (*e.g.*, Beus 1962, 1966, Dunn 1976, Burt 1980) in quartz–greisen veins (*e.g.*, Cornwall, U.K.) and in skarn deposits (*e.g.*, Iron Mountain, New Mexico). Danalite has been reported in western Tasmanian skarn deposits (*e.g.*, Mt. Lindsay: Kwak 1983; Cleveland: Barth 1986; Pine Hill and St. Dizier: W.H. Barth, pers. comm., 1987). The Mt. Lindsay danalite is close to an end-member composition ($Dan_{89.2}Hel_{8.7}Gen_{2.1}$; Kwak 1983).

Helvite also occurs in syenite pegmatites of the Oslo region, Norway (Larsen 1988). Clark & Fejer (1976) reported the occurrence of genthelvite in the Cairngorm Mountains, Scotland. In a review of the occurrence of helvite-group minerals from various localities, Dunn (1976) stated that end-member danalite is not recorded in natural occurrences, and that a compositional gap exists between the Zn and Mn end-members. However, Perez *et al.* (1990) documented the occurrence of a composition intermediate between the Zn and Mn end-members from the Taghouaji Complex, Niger. Raimbault & Bilal (1993) recently reported trace-element contents of helvite-group minerals from Brazil and China.

The compositions of helvite from Rosebery are plotted together with those from other localities on Figure 9. They are more Mn-rich than those from the Cleveland mine, and are compositionally distinct from the genthelvite from Cairngorm, Scotland, and the Mn-rich helvite with a minor genthelvite component from Oslo, Norway (Fig. 9).

Among natural occurrences, the maximum recorded danalite component is only 87 mol.% (Dunn 1976). Danalite has not yet been synthesized (Burt 1980), which suggests that the pure end-member is probably unstable. Burt (1980) suggested the following two reactions for equilibration of danalite with pyrite, pyrrhotite, hematite, and magnetite.

$$6 \text{ hematite} + 2 \text{ danalite} = \text{pyrite} + 6 \text{ magnetite} + 3 \text{ phenakite} + \text{quartz} \quad (1)$$

$$3 \text{ pyrite} + 4 \text{ danalite} = 10 \text{ pyrrhotite} + 3 \text{ magnetite} + 6 \text{ phenakite} + 6 \text{ quartz} \quad (2)$$

Helvite-group minerals from Cleveland and Mt. Lindsay contain a significant danalite component, and the material from the F(J) lens at Rosebery contains up to 55.7 mol.% danalite.At Rosebery, the helvite occurs in association with magnetite, pyrrhotite and pyrite, and not with hematite, suggesting that a reaction closer to (2) controlled the helvite equilibrium, even though phenakite has not been identified in the F(J) lens.

Burt (1980) demonstrated that danalite is stable under more sulfidizing conditions than pyrrhotite, and more oxidizing conditions than fayalite. Danalite is sensitive to hypogene oxidation, whereas helvite and genthelvite are sensitive to S–O exchange [*i.e.*, variation in log $f(O_2)/f(S_2)$], as expressed in the following reactions:

$$6 \text{ danalite} + 7\ O_2 = 8 \text{ magnetite} + 9 \text{ phenakite} + 9 \text{ quartz} + 3\ S_2 \quad (3)$$

$$2 \text{ danalite} + 8\ S_2 = 8 \text{ pyrite} + 3 \text{ phenakite} + 6 \text{ quartz} + 4\ O_2 \quad (4)$$

$$2 \text{ danalite} + 4\ S_2 = 8 \text{ pyrrhotite} + 3 \text{ phenakite} + 8 \text{ quartz} + 4\ O_2 \quad (5)$$

Under increasing CO_2 pressure, danalite breaks down according to the following reaction:

TABLE 4. REPRESENTATIVE COMPOSITIONS OF BIOTITE, F(J) LENS, ROSEBERY MINE, TASMANIA

Sample no.	R1920		88R		R3024		R3023		R3492		R3033R1477	
	-12	-6	-3A	-4A	-3A	-3C	-8	-2	-17	-28	-27	-11
	(4)	(6)	(2)	(3)	(4)	(6)	(4)	(3)	(3)	(7)	(3)	(2)
Section	100mS		200mS		220mS		270mS		280mS		300mS	
SiO_2 wt.%	36.61	34.94	36.25	33.93	39.69	39.01	37.11	37.74	38.05	38.59	36.98	42.23
TiO_2	0.79	0.33	1.02	0.56	0.49	0.85	0.44	0.87	0.17	0.38	0.31	0.89
Al_2O_3	16.15	16.35	15.69	18.29	15.35	21.76	13.24	17.66	11.91	12.33	12.80	29.82
FeO	24.72	27.05	25.96	24.99	19.35	23.71	25.79	23.99	23.52	24.62	28.36	8.43
MnO	0.91	1.54	0.85	0.76	0.77	0.42	0.52	0.24	0.27	0.85	0.44	0.76
MgO	5.54	6.37	5.93	6.80	10.02	4.55	9.33	6.64	11.96	10.42	7.82	5.61
CaO	n.d.	n.d.	n.d.	n.d.	n.d.	0.05	n.d.	n.d.	n.d.	n.d.	n.d.	0.08
K_2O	8.62	8.37	8.72	8.82	7.76	5.43	8.89	8.45	8.71	9.04	8.61	7.61
Cl	0.18	0.31	0.20	0.26	0.03	0.03	0.21	n.d.	0.24	0.15	0.20	n.d.
Total	93.52	95.26	94.62	94.41	93.46	95.81	95.53	95.59	94.83	96.38	95.52	95.43
Number of ions on the basis of 22 atoms of oxygen												
^{IV}Al	2.17	2.44	2.26	2.70	1.92	2.23	2.18	2.23	2.09	2.04	2.13	2.17
Si	5.84	5.56	5.75	5.30	6.08	5.77	5.83	5.77	5.91	5.96	5.87	5.83
Ti	0.10	0.04	0.12	0.07	0.06	0.10	0.05	0.10	0.02	0.05	0.04	0.10
^{VI}Al	0.87	0.62	0.66	0.67	0.82	1.57	0.25	0.94	0.09	0.21	0.13	2.68
Fe^{2+}	3.33	3.61	3.30	3.27	2.51	2.97	3.39	3.08	3.05	3.19	3.77	0.97
Mn	0.12	0.21	0.11	0.10	0.08	0.05	0.07	0.03	0.03	0.11	0.06	0.09
Mg	1.32	1.51	1.40	1.58	1.94	1.01	2.19	1.52	2.77	2.40	1.85	1.15
Ca	-	-	-	-	-	0.01	-	-	-	-	-	0.01
K	1.75	1.70	1.77	1.76	1.38	1.02	1.79	1.65	1.72	1.79	1.74	1.34
Cl	0.05	0.09	0.06	0.06	0.01	0.01	0.06	-	0.06	0.05	0.05	-
Σ Cations	15.55	15.78	15.43	15.51	14.80	14.74	15.81	15.32	15.74	15.80	15.64	14.34
Mg/(Mg+Fe)	0.28	0.30	0.30	0.33	0.44	0.26	0.39	0.33	0.48	0.43	0.33	0.54

The number of electron-microprobe analyses carried out is shown in parentheses. n.d.: not detected.

$$2\ \text{danalite} + CO_2 = 6\ \text{siderite} + 3\ \text{phenakite} + 3\ \text{quartz} + 2\ \text{pyrrhotite} \quad (6)$$

The presence of CO_2 in the F(J) lens has been confirmed in fluid-inclusion studies (Khin Zaw 1991). H_2O–CO_2-bearing and CO_2-liquid-bearing fluid inclusions are abundant in quartz, fluorite, and helvite. However, because thermodynamic data are not available for all phases in reaction 6, absolute constraints on $f(O_2)$–$f(S_2)$–$f(CO_2)$ cannot be made on the basis of observed assemblages of minerals.

Despite this limitation, the occurrence of helvite together with fluorite in the F(J) lens of the Rosebery mine indicates that Be was introduced with fluorine during the replacement process, which accumulated in the form of helvite in silicate-poor ore enriched in magnetite, pyrite, and pyrrhotite.

Biotite

Electron-microprobe data for biotite from Rosebery (Table 4) are plotted in Figure 11 (after Deer *et al.* 1962). The biotite contains 7.2–9.2 wt% K_2O; however, altered biotite may contain as little as 3.8 wt% K_2O. Analyses across a single grain show that K and Fe increase from core to rim. Both green and brown varieties in sample R3492–28 were analyzed, but no significant variations in Ti or Fe were observed.

Biotite displays a significant variation in Fe content, with values between 19.7 and 31.4 wt% FeO, and it contains between 14.1 and 15.8 total cations. As the calculations of stoichiometry assume only Fe^{2+}, the higher cation totals suggest the presence of Fe^{3+}. Biotite displays a range of ^{IV}Al (1.81–2.73), ^{VI}Al (0.02–2.75), and 100Mg/(Mg + Fe^{2+}) values (22.2 to 54.1) (Fig. 11).

The compositional variations can be used to distinguish different modes of occurrence (*e.g.*, magmatic *versus* metasomatic origin in porphyry copper and skarn environments). Hydrothermal biotite in porphyry copper deposits is more magnesian than magmatic biotite in the host intrusive stock (Beane 1974, 1982, Jacobs & Parry 1976). At the CanTung mine, the biotite in the skarns is more Mg-rich than magmatic biotite in the nearby granitic stock (Khin Zaw 1976, Khin Zaw & Clark 1978).

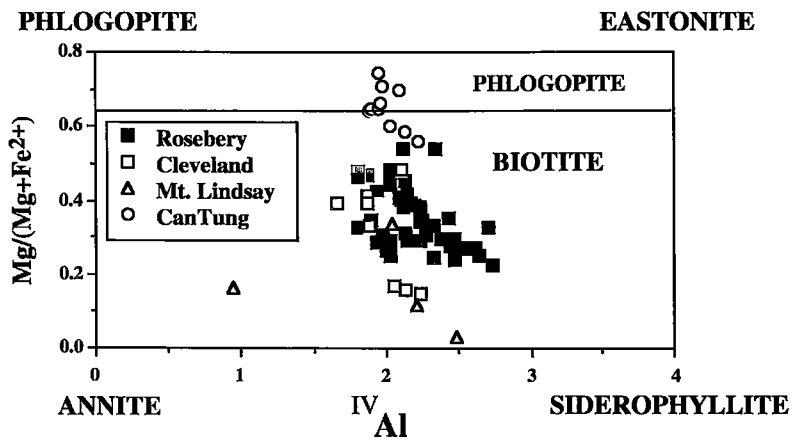

FIG. 11. Plot of Mg/(Mg + Fe^{2+}) *versus* ^{IV}Al for biotite from Rosebery, together with compositional variation of biotite from Mt. Lindsay and Cleveland, western Tasmania (Kwak 1983, Barth 1986), and biotite from the CanTung mine, Northwest Territories (Khin Zaw 1976).

TABLE 5. REPRESENTATIVE COMPOSITIONS OF TOURMALINE, F(J) LENS, ROSEBERY MINE, TASMANIA

Sample no.	R1920 -12 (5)	88R -6 (9)	88R -4A (5)	88R -10 (4)	R3023 -8 (1)	17L -KZ (4)	R3033 -29 (3)	R3492 -17 (7)	R3024 -3A (2)	82R -7B (1)
SiO_2 wt.%	36.77	34.63	34.05	36.00	36.07	34.20	35.61	34.56	35.86	34.83
TiO_2	0.32	0.06	0.32	n.d.	0.18	0.17	0.90	0.20	n.d.	n.d.
Al_2O_3	31.33	29.78	27.04	33.27	28.06	26.98	25.37	23.82	31.04	27.64
FeO	14.36	16.41	15.35	10.48	18.03	16.42	20.93	22.20	13.24	22.86
MnO	n.d.	0.17	n.d.	n.d.	n.d.	0.07	0.07	n.d.	n.d.	n.d.
MgO	3.79	3.16	3.87	4.51	4.05	4.43	3.23	3.73	3.91	1.54
CaO	0.12	0.27	0.55	0.26	0.27	0.56	0.31	0.29	0.08	0.19
Na_2O	2.41	2.50	2.27	1.90	2.68	2.37	2.74	2.55	2.07	2.46
K_2O	n.d.	0.09	n.d.	n.d.	n.d.	0.04	0.05	0.14	0.06	0.14
Total	89.10	87.07	83.45	86.42	89.34	85.24	89.21	87.49	86.26	89.66
	Number of ions on the basis of 29 atoms of oxygen									
T site										
Si	6.02	5.92	6.03	5.94	6.05	6.00	6.11	6.11	6.04	5.98
^{IV}Al	0.01	0.08	0.00	0.06	0.00	0.01	0.00	0.01	0.00	0.02
Z site										
^{VI}Al	5.95	5.90	5.65	6.00	5.55	5.56	5.12	4.96	6.00	5.58
Y site										
^{VI}Al	0.09	0.01	0.00	0.42	0.00	0.00	0.00	0.00	0.15	0.00
Ti	0.04	0.01	0.04	0.00	0.02	0.02	0.12	0.03	0.00	0.00
Fe^{2+}	1.97	2.35	2.28	1.46	2.53	2.41	3.00	3.29	1.87	3.28
Mn	0.00	0.02	0.08	-	0.00	0.01	0.01	-	-	-
Mg	0.93	0.81	1.02	1.11	1.01	1.16	0.83	0.98	0.98	0.39
X site										
Ca	0.02	0.05	0.11	0.05	0.05	0.10	0.06	0.05	0.02	0.04
Na	0.77	0.83	0.78	0.61	0.87	0.81	0.91	0.88	0.68	0.82
K	-	0.02	-	-	-	0.01	0.01	0.03	0.01	0.03
Σ Cations	15.80	16.00	15.99	15.65	16.08	16.09	16.17	16.34	15.75	16.14
Fe/(Fe + Mg)	0.68	0.74	0.69	0.57	0.72	0.68	0.78	0.77	0.66	0.89

The number of electron-microprobe analyses carried out is shown in parentheses. n.d.: not detected.

In Figure 11, the compositions of biotite at Rosebery are compared with those of the Cleveland tin deposit, and of typical, high-temperature, W- and biotite-bearing skarns from CanTung (Khin Zaw 1976). Barth (1986) demonstrated that biotite from the Cleveland replacement deposit yields a range in $100Mg/(Mg + Fe^{2+})$ of 15.8 to 48.3; skarn biotite from Mt. Lindsay displays a range of $100Mg/(Mg + Fe^{2+})$ from 3.3 to 33.4 (Kwak 1983). The biotite composition at Rosebery is comparable with those from the Mt. Lindsay and Cleveland deposits, but distinct from those of high-temperature skarn deposits. The distinction is consistent with a low to moderate temperature of formation.

Tourmaline

Tourmaline occurs in a wide range of geological environments, including sedimentary, metasomatic, and granitic–magmatic. Plimer & Lees (1988) analyzed tourmaline from tourmalinites and from joint- and fracture-fillings in the south end of the Rosebery deposits, and from Devonian granites in western Tasmania. In this study, we analyzed the tourmaline in ten samples from the F(J) lens (Table 5). Plots in terms of Al–Fe–Mg and Mg–Fe–Ca (Figs. 12, 13) indicate that at Rosebery, the tourmaline consists predominantly of schorl rather than dravite or elbaite. No systematic compositional zonation in the tourmaline was recorded.

Plimer & Lees (1988) analyzed two samples of tourmaline each from the Meredith granite (Cleveland) and the Heemskirk granite. They found the tourmaline to be exclusively schorl, on the Al–Fe join of the Al–Fe–Mg diagram and at the Fe-end of the Fe–Mg–Ca plot. In contrast, Barth (1986) analyzed a large number of tourmaline samples from the Meredith granite and recognized significant Mg contents.

The compositions of tourmaline at Rosebery are compared to those from the Meredith granite in Figure 12. Tourmaline compositions from Appalachian–Caledonian massive sulfide deposits (Taylor & Slack 1984) and from the Kidd Creek volcanogenic massive sulfide deposit, Ontario (Slack & Coad 1989) are compared to material from Rosebery in Figure 13. Tourmaline from Rosebery is similar to that in the Meredith granite, but is significantly more Fe-rich than tourmaline from the Appalachian–Caledonian deposits and most of that from Kidd Creek.

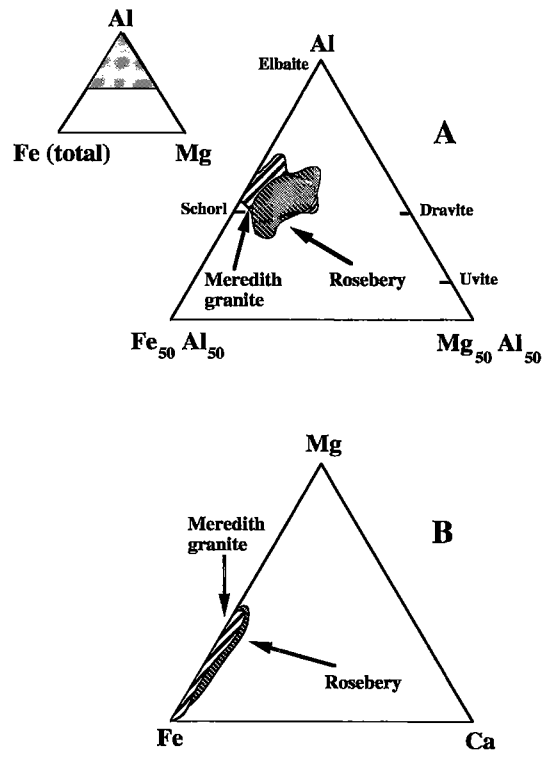

FIG. 12. Al–Fe–Mg plot (A) and Fe–Mg–Ca plot (B) for tourmaline from Rosebery (this study and Plimer & Lees 1988), and for tourmaline from the Devonian Meredith granite (Barth 1986).

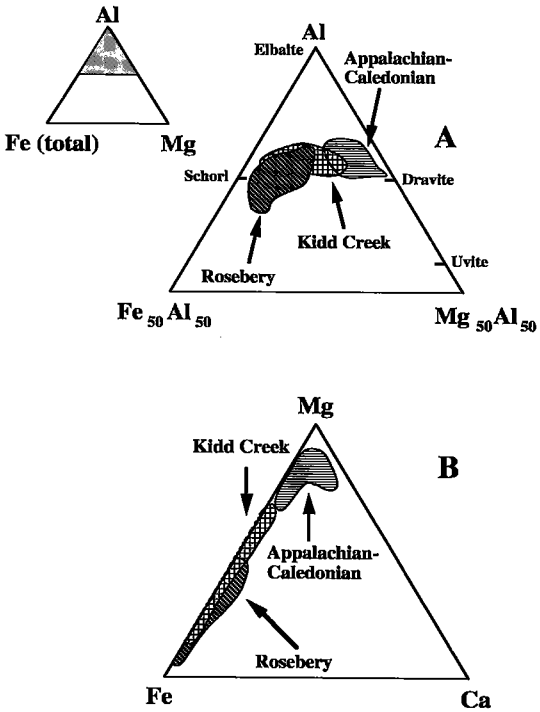

FIG. 13. Al–Fe–Mg plot (A) and Fe–Mg–Ca plot (B) for tourmaline from the F(J) lens, Rosebery, and from Appalachian–Caledonian massive sulfide deposits (Taylor & Slack 1984) and the Kidd Creek volcanogenic massive sulfide deposit (Slack & Coad 1989).

TOURMALINE COMPOSITION AS A METALLOGENIC INDICATOR

In recent years, the compositional variation of tourmaline has attracted attention as a means of inferring the physicochemical environment of associated mineralization. Tourmaline-rich rocks can be found in various environments: (1) granitic–hydrothermal, (2) authigenic, (3) detrital, (4) regional metasomatic, (5) evaporitic–sabkha, and (6) submarine–hydrothermal (Slack 1982). Of these, (2) and (3) are not relevant for the F(J) lens, and (4), which involves the metamorphism of boron-rich illitic clays (Reynolds 1965) or the development of localized veins and segregations of tourmaline by metasomatic replacement in regional metamorphic terranes, is also considered unimportant for the formation of most stratiform tourmaline-rich rocks (Slack 1982).

Certain stratabound mineral deposits, such as those in the Zambian Cu belt (Garlick & Fleischer 1972), are believed to have been deposited under evaporitic or coastal sabkha-type environments, in which boron can accumulate to form a tourmaline-rich rock. However, it is unlikely that environment (5) formed the tourmaline-rich rocks at Rosebery, because the ore lenses are inferred to have formed under a relatively deep-water environment by submarine–exhalative processes (*e.g.*, Green *et al.* 1981, Lees *et al.* 1990). Hence, only environment (1) or (6) could apply; these are evaluated further below.

Tourmaline in a granitic–hydrothermal environment

Tourmaline associated with granites, related pegmatites, aplites, and granite-related veins has long been recognized as a product of late-stage, magmatic–hydrothermal activity. Tourmaline is commonly an important gangue mineral in hydrothermal veins [*e.g.*, tungsten–tin veins at Panasqueira, Portugal (Kelly & Rye 1979), the Mawchi mine, Myanmar (Khin Zaw & Khin Myo Thet 1983)], breccia pipes in the Andes (*e.g.*, Carlson & Sawkins 1980), and porphyry tin deposits in Bolivia (Sillitoe *et al.* 1975).

Enrichment of tourmaline in hydrothermal veins and breccias has led some to speculate that boron may be involved in metal transport (*e.g.*, Charoy 1982). However, few experimental data exist on the speciation of boron complexes, and the solubility of boron in different P – T – *X* fluids is poorly known. Recently, the composition (*e.g.*, major and trace elements, including the *REE*) of tourmaline has been used to better interpret the evolution and cooling history of granite and pegmatite bodies (Manning 1982, London 1986, Jolliff *et al.* 1986, 1987), and the formation of Archean lode gold deposits (King & Kerrich 1986). Tourmaline occurs primarily in western Tasmania in association with granites (*e.g.*, the Heemskirk granite and Meredith granite) and related carbonate-replacement tin ± tungsten deposits (*e.g.*, Renison Bell, Cleveland, Mt. Bischoff).

Tourmaline in a submarine–hydrothermal environment

Tourmaline in submarine-hydrothermal ores has been interpreted to form by the same exhalative processes on the seafloor that formed the associated massive sulfide deposits (*e.g.*, Slack 1982, Taylor & Slack 1984, Slack *et al.* 1984, 1993, Plimer 1988, Slack & Coad 1989). Tourmaline in Appalachian–Caledonian massive sulfide deposits is found as disseminations, clots, and fracture fillings in massive sulfide bodies and adjacent wallrocks and, in some areas, as stratiform layers composed of massive foliated tourmaline, commonly referred to as "tourmalinite" (Slack 1982, Slack *et al.* 1984).

Stratabound tourmaline also is reported from the sediment-hosted Sullivan Pb–Zn–Ag massive sulfide deposit, British Columbia (*e.g.*, Ethier & Campbell 1977, Beaty *et al.* 1988), the Broken Hill Pb–Zn–Ag deposit, New South Wales, and the Golden Dyke Dome Au deposit, Northern Territory (Plimer 1983, 1986). Stratabound tourmalinite also was recently reported as

a distal equivalent of the Proterozoic Starra Au–Cu deposit, Queensland (Davidson 1989). Tourmalinite of possible exhalative origin has also been described in association with Pb–Zn–Ag mineralization at Bottino, Apuane Alps, Italy (Benvenuti *et al.* 1989, 1991).

Slack (1982) and Taylor & Slack (1984) considered tourmalinite to be facies equivalents of exhalative sulfide lenses, and demonstrated that in most cases, the tourmaline associated with massive sulfide deposits is dravite, in contrast to the schorl typical of felsic plutonic associations. However, later studies of the tourmaline at Kidd Creek by Slack & Coad (1989) documented a wide range of compositions, from Fe-rich dravite nearly to end-member schorl, with Fe/(Fe + Mg) varying from 0.33 to 0.92. Plimer (1983) showed that tourmaline in the Broken Hill district, Australia, is relatively Fe-rich, although that intergrown with Fe-sulfide minerals is moderately Mg-rich (Slack *et al.* 1993).

Genetic significance of tourmaline at Rosebery

Plimer & Lees (1988) analyzed tourmaline from banded "tourmalinite" samples at Rosebery and reported Fe/(Fe + Mg) values of 0.6 to 0.8, whereas joint-filling tourmaline was found to have an Fe/(Fe + Mg) value of 0.7 to 0.8. Electron-microprobe data on tourmaline from the south end of the Rosebery mine reported here yield a range of Fe/(Fe + Mg) from 0.5 to 0.9.

On an Al–Fe–Mg plot, the four tourmalinite samples by Plimer & Lees (1988) display nearly identical compositions to the tourmaline samples from Rosebery. The Fe–Mg–Ca plot also indicates similar compositional ranges. Hence, both the banded tourmalinites and the fracture-filling tourmaline at Rosebery are likely to be products of the same hydrothermal process. Previously reported differences in composition between these two types of sample are probably due to random statistical differences related to the small number of samples characterized by Plimer & Lees (1988).

Plimer & Lees (1988) concluded that at Rosebery, tourmaline compositions define two distinct groupings: (1) tourmalinite of submarine-hydrothermal origin, and (2) tourmaline related to a Devonian granite. In their opinion, tourmaline found in 3–5-cm-thick layers, known as "tourmalinite" in underground exposures (*e.g.*, 15 Level), formed by submarine chemical precipitation as tourmaline exhalites. Plimer & Lees (1988, p. 100) stated that "late in the history of the formation of the Rosebery deposit, temperatures were low enough and the Eh and pH were high enough to allow tourmaline precipitation from a fluid with a high activity of boron. Debouchment of boron-bearing ore fluids earlier in the submarine hydrothermal history would have resulted in infinite dilution of boron in seawater. Replacement of earlier assemblages in the fluid conduit by late stage tourmaline is envisaged with maximum tourmaline precipitation as an exhalite shortly after deposition of the massive sulphides. Because tourmaline is the only possible precursor mineral to the tourmaline in the exhalites, it is suggested that the primary precipitate from the submarine hot fluid was a gel from which tourmaline, silica, iron oxides and iron sulphides precipitated."

The following features are considered inconsistent with a submarine-exhalative origin of the tourmaline at Rosebery:

(1) Detailed examination of the underground exposures of tourmalinite (*e.g.*, 15 Level) clearly indicates that the tourmaline assemblages cut across the Devonian cleavage (Fig. 5H).

(2) Detailed investigation of the tourmalinite does not reveal any evidence for predeformation textures. Tourmaline assemblages lack sedimentary textures such as graded bedding or cross-lamination. Tourmalinite clasts also are unknown from the Rosebery–Hercules area.

(3) The occurrences of "bedded" tourmalinite of Plimer & Lees (1988) are localized, without stratigraphic continuity, in contrast to tourmalinites in other stratabound massive sulfide environments (Slack *et al.* 1984, 1993) that may be traceable for more than a kilometer along strike.

(4) Tourmaline is not present in other VHMS deposits in the Mt. Read volcanic belt, and tourmaline is only recognized at Rosebery where there is strong geophysical evidence for a body of Devonian granite at shallow depth beneath the southern end of the deposit.

(5) No sedimentary sequences of evaporitic origin have been reported in the Mt. Read volcanic belt that could have supplied abundant boron during convective circulation of hydrothermal fluids to form the tourmaline.

Barth (1986) obtained extensive electron-microprobe data on tourmaline from the Meredith granite south of Cleveland, including vein tourmaline and accessory tourmaline from the host sandstones. The tourmaline compositions from the Meredith granite are not strictly schorl in composition, but contain a minor component of dravite. This is consistent with the compositional ranges observed in granitic rocks elsewhere (*e.g.*, Neiva 1974, Manning 1982, Taylor *et al.* 1992).

At Kidd Creek, tourmaline is locally zoned from an Fe-rich core to an Mg-rich rim. Slack & Coad (1989) proposed that this chemical zoning and a deposit-scale zoning of average compositions of tourmaline cores are due to mixing between high-temperature, Fe-rich hydrothermal fluid and cold, Mg-rich entrained seawater, causing systematic changes in the Fe/(Fe + Mg) values. No such chemical variations have been observed in the Rosebery material.

The tourmaline from Rosebery and that from the Meredith granite display similar ranges in composition

(Fig. 12). This chemical similarity suggests that the tourmaline from Rosebery formed by granite-related hydrothermal activity. This conclusion is consistent with the inferred existence of a shallow granite intrusion below the south-end orebody.

Composition of chlorite in the Rosebery deposit

The compositional variation of chlorite from the D, G, and H lenses of the Rosebery mine was investigated by Green *et al.* (1981) and Green (1983). In this study, chlorite grains from the F(J) lens were analyzed with an electron microprobe; analytical data are listed in Table 6. Chlorite in the F(J) lens displays variations in SiO_2 (23.6–25.5 wt%), Al_2O_3 (18.5–19.8 wt%), FeO (32.9–39.8 wt%), MnO (1.1–2.6 wt%), and MgO (4.6–9.1 wt%); K_2O and CaO contents are uniformly less than 1.0 wt%. The highest K_2O content (0.74 wt%) is found in chlorite associated with biotite. This high content probably reflects fine-scale intergrowths of biotite or muscovite (J. Slack, pers. comm., 1995). Electron-microprobe analyses across single grains of chlorite indicate a lack of significant compositional variations. On a cation basis, the chlorite compositions have Fe/(Fe + Mg) values in the range 0.39–0.83, and Si values in the range 5.08–5.66 atoms per formula unit. In the chemical classification of Hey (1954), these compositions correspond to daphnite, ripidolite, and brunsvigite (Fig. 14).

TABLE 6. REPRESENTATIVE COMPOSITIONS OF CHLORITE, F(J) LENS, ROSEBERY MINE, TASMANIA

Sample no.	R3024 -3A (3)	R3492 -28 (2)	R3023 -2 (4)	R3024 -3C (7)	R1477 -11 (8)	81R -10 (8)
SiO_2 wt.%	24.92	24.19	23.68	24.58	25.41	24.38
TiO_2	n.a.	n.a.	n.a.	n.a.	0.09	n.a.
Al_2O_3	18.34	18.95	19.45	18.88	20.81	22.64
FeO	33.00	38.05	38.40	38.99	20.48	31.64
MnO	2.40	2.20	1.19	1.47	2.08	1.30
MgO	9.15	5.39	5.02	4.96	16.90	7.90
CaO	n.d.	0.44	n.d.	n.d.	n.d.	n.d.
K_2O	n.d.	n.d.	0.18	0.28	0.38	0.21
Total	87.81	89.22	87.92	89.16	86.15	88.07
Number of ions on the basis of 28 atoms of oxygen						
Si	5.56	5.46	5.42	5.56	5.39	5.33
^{IV}Al	2.45	2.54	2.59	2.45	2.61	2.68
Ti	-	-	-	-	0.02	-
^{VI}Al	2.38	2.50	2.66	2.58	2.60	3.15
Al	4.82	5.04	5.25	5.02	5.21	5.83
Fe^{2+}	6.16	7.18	7.34	7.37	3.64	5.78
Mn	0.46	0.42	0.23	0.28	0.38	0.25
Mg	3.05	1.82	1.71	1.68	5.35	2.57
Ca	-	0.11	-	-	-	-
K	-	-	0.05	0.08	0.05	0.06
Σ Cations	20.06	20.03	20.00	20.00	20.04	19.82
Fe/(Fe + Mg)	0.67	0.80	0.81	0.81	0.40	0.69
Correction	0.47	0.56	0.57	0.57	0.28	0.48
Temperature 1	277.6	287.8	292.6	277.7	294.4	302.0
Temperature 2	274.0	-	-	-	298.5	308.5
$f(O_2)$	–33.1	-	-	-	–31.1	–30.3
$f(H_2S)$	–0.8	-	-	-	–1.3	–0.8

Temperature 1 was calculated with the chlorite geothermometer developed by Cathelineau & Nieva (1985). Temperature 2, $f(O_2)$ and $f(H_2S)$ were calculated with the six-component chlorite solution model of Walshe (1986), provided by G.R. Green of the Tasmanian Mines Department. Note that chlorine was sought, but not detected. n.a.: not analyzed, n.d.: not detected. The number of electron-microprobe analyses carried out is shown in parentheses.

Comparison with chlorite in VHMS deposits

Compositional variations of chlorite in volcanogenic massive sulfide deposits have been studied extensively [*e.g.*, Mt. Lyell deposit, western Tasmania: Hendry (1981), South Bay deposit, Ontario: Urabe & Scott (1983), Bruce deposit, Arizona: Larson (1984), Phelps Dodge deposit, Quebec: Kranidiotis & MacLean (1987)]. Slack & Coad (1989) analyzed chlorite from the Kidd Creek deposit; their compositions are shown with those from the F(J) lens (Table 6) and from D, G, and H lenses (Green *et al.* 1981, Green 1983) in Figure 14.

The chlorite compositions from the D, G, and H lenses vary in Fe/(Fe + Mg) value from 0.67 to 0.86, with Si values from 5.05 to 5.31, and fall in the fields of daphnite and ripidolite. Chlorite compositions from Kidd Creek display Fe/(Fe + Mg) values in the range 0.43–0.98, and Si values in the range 5.00–5.39, and are similar to chlorite of the D, G, and H lens. In comparison, chlorite in the F(J) lens seems to be somewhat more siliceous, with Si values up to 5.7.

Chlorite geothermometry

Walshe & Solomon (1981) and Walshe (1986) developed a thermodynamic model using the six-component solid-solution series of chlorite to provide estimates of physicochemical conditions such as T, $f(O_2)$, $f(S_2)$, and $a(H_2S)$ in the hydrothermal environment. Reed (1984), Cathelineau & Nieva (1985), and Shikazono & Kawahata (1987), among others, suggested that the composition of chlorite can be used as an indicator of hydrothermal conditions.

Cathelineau & Nieva (1985) analyzed the composition of chlorite and measured the temperatures from deep drill-holes in a geothermal system in Mexico. They found that ^{IV}Al of the chlorite increases with increasing temperature. The chlorite used to calibrate their empirical geothermometer came from a maximum depth of 2500 m. In this study, temperatures of formation of the F(J) lens chlorite, calculated using the method of Cathelineau & Nieva (1985), yield a range of 267–328°C (mean: 297°C).

The thermodynamic model of Walshe (1986) also was applied to the compositional data for chlorite from the F(J) lens to calculate temperatures of formation. Calculations for an assumed pressure of 1 kbar produced only ten solutions for the 32 compositions of chlorite. The range, 270–352°C (mean: 311°C) obtained

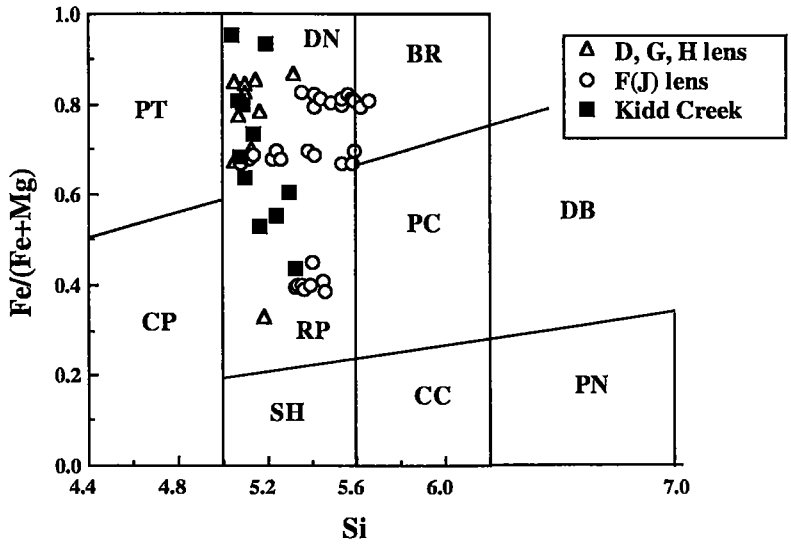

FIG. 14. Compositions of chlorite from the F(J) lens, Rosebery, and the Kidd Creek volcanogenic massive sulfide deposit (Slack & Coad 1989). Field boundaries after Hey (1954). Abbreviations: PT pseudothuringite, CP corundophilite, DN daphnite, RP ripidolite, SH sheridanite, BR brunsvigite, PC pycnochlorite, CC clinochlore, DB diabanite, PN penninite.

by Walshe's thermodynamic model compares favorably with the results obtained using the empirical geothermometer of Cathelineau & Nieva (1985).

The accuracy of the above two geothermometers is unknown, as is the effect of pressure. Fluid-inclusion studies indicate homogenization temperatures up to 330°C (Khin Zaw 1991, Khin Zaw *et al.* 1997). The fluid-inclusion results are more similar to the temperatures calculated using Walshe's (1986) chlorite model. Walshe's program has been used to estimate a range of $f(O_2)$ (–27.3 to –33.5) and $a(H_2S)$ (–0.5 to –1.33) values for the formation of chlorite in the the F(J) lens.

The temperature and $\log f(O_2)$ data seem to indicate a linear relationship, as noted for chlorite from the Koonya prospect, 3 km along strike to the south of Rosebery (Hall 1990). However, it is uncertain whether the temperatures estimated by chlorite geothermometry represent formation during the Cambrian, or during the later Devonian metasomatic overprint. Texturally, chlorite is in equilibrium with metasomatic minerals (*e.g.*, biotite, magnetite, pyrrhotite, tourmaline); it is, therefore, most likely that the calculated temperatures reflect the Devonian event.

SERICITE AND K-FELDSPAR AT ROSEBERY

The sericite in the F(J) lens is phengitic, with FeO contents of 0.1–5.4 wt%. Green *et al.* (1981) reported similar compositions from the G, H, and F lenses, except for generally lower FeO contents (1.6–3.9 wt%). The higher FeO contents of phengite in the F(J) lens, compared to the phengite in the stratiform G, H, and F lenses, is probably due to iron enrichment during the Devonian metasomatic event. Hendry (1981) analyzed phengite from the Mt. Lyell volcanic-rock-hosted copper deposit and found between 0.4 and 3.0 wt% FeO. Hendry (1981) interpreted such phengite to be a product of the reaction of silicates with Fe-bearing sulfides and oxides (pyrite and magnetite) during the Devonian event. The presence of coexisting sericite and K-feldspar in the F(J) lens suggests that this replacement process occurred under conditions of moderate pH.

CONCLUDING REMARKS

Brathwaite (1974) initially interpreted the pyrrhotite – pyrite-bearing assemblages that transgress the stratiform sulfide lenses in the south end of the Rosebery mine as products of Devonian metamorphism. Since that study, drilling and geological investigation have indicated that the transgressive assemblages actually include a wide variety of other minerals, such as garnet, helvite, and tourmaline. Later investigators attributed the Fe–S–O and silicate mineral assemblages to hydrothermal activity associated with a post-kinematic Devonian granite pluton (Solomon *et al.* 1987, Lees 1987, Green & Iliff 1989, Lees *et al.* 1990). Although this granite does not crop out, its existence below the south end of Rosebery has been inferred from gravity data (Leaman & Richardson 1989).

The geological, petrological, and geochemical criteria outlined in this study support a metasomatic replacement origin for the transgressive mineral assemblages rather than an origin by isochemical metamorphism or syngenetic deposition. Minerals such as biotite, garnet, helvite, and tourmaline found in the south-end Fe–S–O zones are characteristic of other well-documented granite-related replacement deposits of Devonian age in western Tasmania (*e.g.*, Mt. Lindsay: Kwak 1983, Cleveland: Collins 1981, Barth 1986).

Acknowledgements

We thank geologists at the Rosebery mine for discussions and assistance at the mine site. We also thank Ron Berry, Stuart Bull, David Cooke, Garry Davidson, Bruce Gemmell, Richard Keele, Jocelyn McPhie, Peter McGoldrick and Joe Stolz at the Key Centre for Ore Deposit and Exploration Studies (CODES) at the University of Tasmania for discussions. David Cooke read an earlier version of the manuscript and made valuable suggestions. The authors are indebted to Ron Berry of CODES and Domingo Aerden of Universidad de Salamanca for discussions concerning structural relationships at Rosebery. We also thank various staff members of the Tasmanian Department of Mines and Energy for constructive discussions, particularly Geoff Green, who helped with application of John Walshe's computer program. Special thanks are due to John Slack for his incisive and constructive comments. June Pongratz and Debbie Harding drafted the diagrams.

References

Adams, R.L., Burton, C.C.J., Druett, J.G., Hanson, N.H. & McNaught, I.S. (1976): The Rosebery and Hercules zinc–lead deposits. *In* Ore Deposits of Western Tasmania. *Int. Geol. Congress, 25th (Sydney), Excursion Guide* **31AC**, 31-36.

Aerden, D.A.M. (1991): Foliation-boudinage control on the formation of the Rosebery Pb–Zn orebody, Tasmania. *J. Struct. Geol.* **13**, 759-775.

Barth, W.H. (1986): *Geology of the Cleveland Tin Mine, Tasmania, Australia with Special Reference to Mineral Chemistry and Rare Earth Distribution*. Ph.D. thesis, Univ. Heidelberg, Heidelberg, Germany.

Beane, R.E. (1974): Biotite stability in the porphyry copper environment. *Econ. Geol.* **69**, 241-256.

_____ (1982): Hydrothermal alteration in silicate rocks, southwestern North America. *In* Advances in Geology of the Porphyry Copper Deposits of Southwestern North America (S.R. Titley, ed.). University of Arizona Press, Tucson, Arizona (117-137).

Beaty, D.W., Taylor, H.P., Jr. & Coad, P.R. (1988): An oxygen isotope study of the Kidd Creek, Ontario, volcanogenic massive sulfide deposit: evidence for a high ^{18}O ore fluid. *Econ. Geol.* **83**, 1-17.

Benvenuti, M., Costagliola, P., Lattanzi, P. & Tanelli, G. (1991): Mineral chemistry of tourmalines from the Bottino mining district, Apuane Alps (Italy). *Eur. J. Mineral.* **3**, 537-548.

_____, Lattanzi, P. & Tanelli, G. (1989): Tourmalinite-associated Pb–Zn–Ag mineralization at Bottino, Apuane Alps, Italy: geologic setting, mineral textures, and sulfide chemistry. *Econ. Geol.* **84**, 1277-1292.

Berry, R.F. (1990): The structure of the Rosebery mine sequence, western Tasmania. *In* Gondwana: Terranes and Resources. *Tenth Australian Geological Convention Hobart), Geol. Soc. Aust., Abstr.* **25**, 278-279.

Beus, A.A. (1962): *Beryllium. Evaluation of Deposits during Prospecting and Exploratory Work.* Freeman, San Francisco, California.

_____ (1966): *Geochemistry of Beryllium and Genetic Types of Beryllium Deposits*. Freeman, San Francisco, California.

Brathwaite, R.L. (1969): *The Geology of the Rosebery Ore Deposits*. Ph.D. thesis, Univ. Tasmania, Hobart, Australia.

_____ (1972): The structure of the Rosebery ore deposit, Tasmania. *Proc. Austral. Inst. Mining Metall.* **241**, 1-13.

_____ (1974): The geology and origin of the Rosebery ore deposit, Tasmania. *Econ. Geol.* **69**, 1086-1101.

Burt, D.M. (1980): The stability of danalite, $Fe_4Be_3(SiO_4)_3S$. *Am. Mineral.* **65**, 355-360.

Burton, C.C.J. (1975): Rosebery zinc–lead–copper orebody. *In* Economic Geology of Australia and Papua New Guinea. 1. Metals (C.L. Knight, ed.). The Australasian Inst. Mining Metall., Melbourne, Australia (619-626).

Carlson, S.R. & Sawkins, F.J. (1980): Mineralogic and fluid inclusion studies of the Tourmalina Cu–Mo-bearing breccia pipe, northern Peru. *Econ. Geol.* **75**, 1233-1238.

Cathelineau, M. & Nieva, D. (1985): A chlorite solid solution geothermometer: the Los Azufres (Mexico) geothermal system. *Contrib. Mineral. Petrol.* **91**, 235-244.

Charoy, B. (1982): Tourmalinization in Cornwall, England. *In* Metallization Associated with Acid Magmatism (A.M. Evans, ed.). John Wiley and Sons, Chichester, U.K. (63-70).

Clark, A.M. & Fejer, E.E. (1976): Zoned genthelvite from the Cairngorm Mountains, Scotland. *Mineral. Mag.* **40**, 637-639.

Collins, P.L.F. (1981): The geology and genesis of the Cleveland tin deposit, western Tasmania: fluid inclusion and stable isotope studies. *Econ. Geol.* **76**, 365-392.

CORBETT, K.D. (1981): Stratigraphy and mineralization in the Mt. Read Volcanics, western Tasmania. *Econ. Geol.* **76**, 209-230.

_____ (1992): Stratigraphic-volcanic setting of massive sulfide deposits in the Cambrian Mount Read Volcanics, Tasmania. *Econ. Geol.* **87**, 564-586.

_____ & LEES, T.C. (1987): Stratigraphic and structural relationships and evidence for Cambrian deformation at the western margin of the Mt Read Volcanics, Tasmania. *Aust. J. Earth Sci.* **34**, 45-67.

_____, SOLOMON, M., MCCLENAGHAN, M.P., CARSWELL, J.T., GREEN, G.R., ILIFF, G., HOWARTH, J.W., MCARTHUR, G.J. & WALLACE, D.B. (1989): Cambrian Mt Read Volcanics and associated mineral deposits. *In* Geology and Mineral Resources of Tasmania (C.F. Burrett & E.L. Martin, eds.). *Geol. Soc. Aust., Spec. Publ.* **15**, 84-153.

DAVIDSON, G. (1989): *Starra and Trough Tank: Iron-Formation-Hosted Gold–Copper Deposits of North-West Queensland.* Ph.D. thesis, Univ. Tasmania, Hobart, Australia.

DEER, W.A., HOWIE, R.A. & ZUSSMAN, J. (1962): *Rock-Forming Minerals.* 3. *Sheet Silicates.* Longman, London, U.K.

DUNN, P.J. (1976): Genthelvite and helvite group. *Mineral. Mag.* **40**, 627-636.

EINAUDI, M.T. & BURT, D.M. (1982): Introduction – terminology, classification, and composition of skarn deposits. *Econ. Geol.* **77**, 745-754.

ETHIER, V.G. & CAMPBELL, F.A. (1977): Tourmaline concentrations in Proterozoic sediments of the southern Cordillera of Canada and their economic significance. *Can. J. Earth Sci.* **14**, 2348-2363.

FINUCANE, K.J. (1932): The geology and ore deposits of the Rosebery district. *Chem. Eng. Mining Rev.* **25**, 5-7, 43-46.

FORTEY, N.J. & BEDDOE-STEPHENS, B. (1982): Barium silicates in stratabound Ba–Zn mineralization in the Scottish Dalradian. *Mineral. Mag.* **46**, 63-72.

FRANKLIN, J.M., LYDON, J.W. & SANGSTER, D.F. (1981): Volcanic-associated massive sulfide deposits. *Econ. Geol., 75th Anniv. Vol.*, 485-627.

GARLICK, W.G. & FLEISCHER, V.D. (1972): Sedimentary environment of Zambian copper deposition. *Geol. Mijnbouw* **51**, 277-298.

GREEN, G.R. (1983): *The Geological Setting and Formation of the Rosebery Volcanic-Hosted Massive Sulfide Orebody, Tasmania.* Ph.D. thesis, Univ. Tasmania, Hobart, Australia.

_____ & ILIFF, G. (1989): Rosebery. *In* Geology and Mineral Resources of Tasmania (C.F. Burrett & E.L. Martin, eds.). *Geol. Soc. Aust., Spec. Publ.* **15**, 132-137.

_____, SOLOMON, M. & WALSHE, J.L. (1981): The formation of the volcanic-hosted massive sulfide ore deposit at Rosebery, Tasmania. *Econ. Geol.* **76**, 304-338.

HALL, S. (1990): *The Koonya Prospect, Rosebery, Tasmania.* B.Sc. (Hons) thesis, Univ. Tasmania, Hobart, Australia.

HENDRY, D.A.F. (1981): Chlorites, phengites, and siderites from the Prince Lyell ore deposit, Tasmania, and the origin of the deposit. *Econ. Geol.* **76**, 285-303.

HENRY, D.J. & GUIDOTTI, C.V. (1985): Tourmaline as a petrogenetic indicator mineral: an example from the staurolite-grade metapelites of NW Maine. *Am. Mineral.* **70**, 1-15.

HEY, M.H. (1954): A new review of the chlorites. *Mineral. Mag.* **30**, 277-292.

HUSTON, D.L. (1989): *Aspects of the Geology of Massive Sulphide Deposits from the Balcooma District, Northern Queensland and Rosebery, Tasmania: Implications for Ore Genesis.* Ph.D. thesis, Univ. Tasmania, Hobart, Australia.

_____ & LARGE, R.R. (1988): Distribution, mineralogy and geochemistry of gold and silver in the north-end orebody, Rosebery, Tasmania. *Econ. Geol.* **83**, 1181-1192.

JACOBS, D.C. & PARRY, W.T. (1976): A comparison of the geochemistry of biotite from some Basin and Range stocks. *Econ. Geol.* **71**, 1029-1035.

JOLLIFF, B.L., PAPIKE, J.J. & LAUL, J.C. (1987): Mineral recorders of pegmatite internal evolution: REE contents of tourmaline from the Bob Ingersoll pegmatite, South Dakota. *Geochim. Cosmochim. Acta* **51**, 2225-2232.

_____, _____ & SHEARER, C.K. (1986): Tourmaline as a recorder of pegmatite evolution: Bob Ingersoll pegmatite, Black Hills, South Dakota. *Am. Mineral.* **71**, 472-500.

KELLY, W.C. & RYE, R.O. (1979): Geologic, fluid inclusion, and stable isotope studies of the tin–tungsten deposits of Panasqueira, Portugal. *Econ. Geol.* **74**, 1721-1822.

KHIN ZAW (1976): *The CanTung E-zone Orebody, Tungsten, Northwest Territories: a Major Scheelite Skarn Deposit.* M.Sc. thesis, Queen's University, Kingston, Ontario.

_____ (1991): *The Effect of Devonian Metamorphism and Metasomatism on the Mineralogy and Geochemistry of the Cambrian VMS Deposits in the Rosebery–Hercules District, Western Tasmania.* Ph.D. thesis, Univ. Tasmania, Hobart, Australia.

_____ & CLARK, A.H. (1978): Fluoride–hydroxyl ratios of skarn silicates, CanTung E–zone scheelite orebody, Tungsten, Northwest Territories. *Can. Mineral.* **16**, 207-221.

_____ & KHIN MYO THET, D. (1983): A note on a fluid inclusion study of tin–tungsten mineralization at Mawchi mine, Kayah State, Burma. *Econ. Geol.* **78**, 530-534.

_____, LARGE, R.R. & HUSTON, D.L. (1988): Ore metal distribution, zonation and structural relationships at Rosebery, western Tasmania. Final Consulting report (unpubl.) submitted to Electrolytic Zinc Company of Australasia, University of Tasmania, Hobart, Australia.

_____, _____ & _____ (1997): A chemical model for the Devonian remobilization process in the Cambrian VHMS Rosebery deposit, western Tasmania: constraints from metal zonation, fluid inclusions and thermodynamic calculations. *Econ. Geol.* (in press).

KING, R.W. & KERRICH, R. (1986): Tourmaline in Archean lode gold deposit. *Geol. Soc. Am., Abstr. Programs* **18**, 657.

KRANIDIOTIS, P. & MACLEAN, W.H. (1987): Systematics of chlorite alteration at the Phelps Dodge massive sulfide deposit, Matagami, Quebec. *Econ. Geol.* **82**, 1898-1911.

KWAK, T.A.P. (1983): The geology and geochemistry of the zoned Sn–W–F–Be skarns at Mt Lindsay, Tasmania, Australia. *Econ. Geol.* **78**, 1440-1465.

LARGE, R.R. (1977): Chemical evolution and zonation of massive sulfide deposits in volcanic terrains. *Econ. Geol.* **72**, 549-572.

_____ (1992): Australian volcanic-hosted massive sulfide deposits: features, styles and genetic models. *Econ. Geol.* **87**, 471-510.

LARSEN, A. (1988): Helvite group minerals from syenite pegmatites in the Oslo region, Norway. *Norsk Geol. Tidsskr.* **68**, 119-124.

LARSON, P.B. (1984): Geochemistry of the alteration pipe at the Bruce Cu–Zn volcanogenic massive sulfide deposit, Arizona. *Econ. Geol.* **79**, 1880-1896.

LEAMAN, D.E. & RICHARDSON, R.G. (1989): The granites of west and northwest Tasmania – a geophysical interpretation. *Dep. Mines Tasmania, Geol. Surv. Bull.* **66**.

LEES, T. (1987): *Geology and Mineralization of Rosebery–Hercules Area, Tasmania.* M.Sc. thesis, Univ. of Tasmania, Hobart, Australia.

_____, KHIN ZAW, LARGE, R.R. & HUSTON, D.L. (1990): Rosebery and Hercules copper–lead–zinc deposits. *In* Geology of the Mineral Deposits of Australia and Papua New Guinea (F.E. Hughes, ed.). The Australasian Institute of Mining and Metallurgy, Melbourne, Australia (1241-1247).

LONDON, D. (1986): Formation of tourmaline-rich gem pockets in miarolitic pegmatites. *Am. Mineral.* **71**, 396-405.

LYDON, J.W. (1984): Volcanogenic massive sulfide deposits. 1. A descriptive model. *Geosci. Can.* **11**, 195-202.

_____ (1988): Volcanogenic massive sulfide deposits. 2. Genetic models. *Geosci. Can.* **15**, 43-65.

_____, JONASSON, I.R. & GOODFELLOW, W.D. (1982): Some geochemical aspects of stratiform baritic deposits of Selwyn Basin. *Proc. 11th Int. Congress on Sedimentology*, 18.

MANNING, D.A.C. (1982): Chemical and morphological variation in tourmalines from the Hub Kapong batholith of peninsular Thailand. *Mineral. Mag.* **45**, 139-147.

MATSUKUMA, T., NIITSUMA, H., YUO, S. & WADA, F. (1974): Rare minerals from Kuroko ores of the Uwamaki deposits of the Kosaka mine, Akita Prefecture, Japan. *Mining Geol., Spec. Issue* **6**, 349-361.

MCKENZIE, C.B., DESNOYES, D.W., BARBOUR, D. & GRAVES, R.M. (1993): Contrasting volcanic-hosted massive sulfide styles in the Tulks belt, central Newfoundland. *Explor. Mining Geol.* **2**, 73-84.

MEINERT, L.D. (1983): Variability of skarn deposits: guides to exploration. *In* Revolution in the Earth Sciences – Advances in the Past Half-Century (S.J. Boardman, ed.). Kendall-Hunt Publ. Co., Ames, Iowa (301-316).??

NASCHWITZ, W. (1985): *Geochemistry of the Rosebery Ore Deposit.* Ph.D. thesis, Univ. of Tasmania, Hobart, Australia.

NEIVA, A.M.R. (1974): Geochemistry of tourmaline (schorlite) from granites, aplites and pegmatites from northern Portugal. *Geochim. Cosmochim. Acta* **38**, 1307-1317.

NEWBERRY, R.J. (1983): The formation of subcalcic garnet in scheelite-bearing skarns. *Can. Mineral.* **21**, 529-544.

PEREZ, J., DUSAUSOY, Y., BABKINE, J. & PAGEL, M. (1990): Mn zonation and fluid inclusions in genthelvite from the Taghouaji complex (Air Mountains, Niger). *Am. Mineral.* **75**, 909-914.

PLIMER, I.R. (1983): The association of tourmaline-bearing rocks with mineralisation at Broken Hill, N.S.W. *Proc. Austral. Inst. Mining Metall. Conf. (Broken Hill)* **12**, 157-176.

_____ (1986): Tourmalinites from the Golden Dyke dome, northern Australia. *Mineral. Deposita* **21**, 263-270.

_____ (1988): Tourmalinites associated with Australian Proterozoic submarine exhalative ores. *In* Base Metal Sulfide Deposits in Sedimentary and Volcanic Environments (G.H. Friedrich & P.M. Herzig, eds.). Springer-Verlag, Berlin, Germany (255-283).

_____ & LEES, T. (1988): Tourmaline-rich rocks associated with the submarine hydrothermal Rosebery Zn–Pb–Cu–Ag–Au deposit and granites in western Tasmania, Australia. *Mineral. Petrol.* **38**, 81-103.

RAIMBAULT, L. & BILAL, E. (1993): Trace element contents of helvite-group minerals from metasomatic albitites and hydrothermal veins at Sucuri, Brazil and Dajishan, China. *Can. Mineral.* **31**, 119-127.

REED, M.H. (1984): Geology, wall rock alteration, and massive sulfide mineralization in a portion of the West Shasta district, California. *Econ. Geol.* **79**, 1299-1318.

REYNOLDS, R.C. (1965): Geochemical behaviour of boron during the metamorphism of carbonate rocks. *Geochim. Cosmochim. Acta* **29**, 1101-1114.

SEGNIT, E.R. (1946): Barium-feldspars from Broken Hill, New South Wales. *Mineral. Mag.* **27**, 166-174.

SHIKAZONO, N. & KAWAHATA, H. (1987): Compositional differences in chlorite from hydrothermally altered rocks and hydrothermal ore deposits. *Can. Mineral.* **25**, 465-474.

SHIMAZAKI, Y. (1974): Ore minerals of the Kuroko-type deposits. *Mining Geol., Spec. Issue* **6**, 311-322.

SILLITOE, R.H., HALLS, C. & GRANT, N.J. (1975): Porphyry tin deposits in Bolivia. *Econ. Geol.* **70**, 913-927.

SLACK, J.F. (1982): Tourmaline in Appalachian–Caledonian massive sulphide deposits and its exploration significance. *Inst. Mining Metall. Trans.* **91**, B81-B89.

_____ & COAD, P.R. (1989): Multiple hydrothermal and metamorphic events in the Kidd Creek volcanogenic massive sulphide deposit, Timmins, Ontario: evidence from tourmalines and chlorites. *Can. J. Earth Sci.* **26**, 694-715.

_____ , HERRIMAN, N., BARNES, R.G. & PLIMER, I.R. (1984): Stratiform tourmalinites in metamorphic terranes and their geologic significance. *Geology* **12**, 713-716.

_____ , PALMER, M.R., STEVENS, B.P.J. & BARNES, R.G. (1993): Origin and significance of tourmaline-rich rocks in the Broken Hill district, Australia. *Econ. Geol.* **88**, 505-541.

SOLOMON, M., VOKES, F.M. & WALSHE, J.L. (1987): Chemical remobilization of volcanic-hosted sulfide deposits at Rosebery and Mt. Lyell, Tasmania. *Ore Geol. Rev.* **2**, 173-190.

SPRY, P.G. (1990): Geochemistry and origin of coticules (spessartine–quartz rocks) associated with metamorphosed massive sulfide deposits. *In* Regional Metamorphism of Ore Deposits and Genetic Implications (P.G. Spry & L.T. Bryndzia, eds.). VSP Publ., Zeist, The Netherlands (49-75).

STANTON, R.L. (1972): *Ore Petrology*. McGraw-Hill, New York, N.Y.

STILLWELL, F.L. (1934): Observations on the lead–zinc ore at Rosebery, Tasmania. *Proc. Austral. Inst. Mining Metall.* **94**, 43-67.

TAYLOR, B.E. & SLACK, J.F. (1984): Tourmalines from Appalachian–Caledonian massive sulfide deposits: textural, chemical, and isotopic relationships. *Econ. Geol.* **79**, 1703-1726.

TAYLOR, R.P., IKINGURA, J.R., FALLICK, A.E., HUANG, YIMING & WATKINSON, D.H. (1992): Stable isotope compositions of tourmalines from granites and related hydrothermal rocks of the Karagwe–Ankolean belt, northern Tanzania. *Chem. Geol. (Isotope Geosci.)* **94**, 215-227.

URABE, T. & SCOTT, S.D. (1983): Geology and footwall alteration of the South Bay massive sulphide deposit, northwestern Ontario, Canada. *Can. J. Earth Sci.* **20**, 1862-1879.

WALSHE, J.L. (1986): A six component chlorite solid solution model and the conditions of chlorite formation in hydrothermal and geothermal systems. *Econ. Geol.* **81**, 681-703.

_____ & SOLOMON, M. (1981): An investigation into the environment of formation of the volcanic-hosted Mt. Lyell copper deposits, using geology, mineralogy, stable isotopes, and a six-component chlorite solid solution model. *Econ. Geol.* **76**, 246-284.

WILLIAMS, K.L. (1960): Some less common minerals in the Rosebery and Hercules zinc–lead ores. *Proc. Austral. Inst. Mining Metall.* **196**, 51-59.

Received November 24, 1994, revised manuscript accepted July 15, 1997.